EFFECT OF CYCLIC STRESS RANGE ON CRACK GROWTH OF ALUMINUIM
ALLOY UNDER AXIAL LOADING

MOHAMAD SHAFFAWI BIN ZAINON

A report submitted in partial fulfilment of
The requirements for the award of the degree of
Bachelor of Mechanical Engineering

Faculty of Mechanical Engineering
UNIVERSITI MALAYSIA PAHANG

DECEMBER 2010

AWARD FOR DEGREE

Bachelor Final Year Project Report

Report submitted in partial fulfilment of the requirements for the award of the degree of Bachelor of Mechanical Engineering.

SUPERVISOR'S DECLARATION

I hereby declare that I have checked this project and in my opinion, this project is adequate in terms of scope and quality for the award of the degree of Bachelor of Mechanical Engineering.

Signature

Name of Supervisor: NASRUL AZUAN ALANG

Position: LECTURER OF MECHANICAL ENGINEERING

Date: 6th DECEMBER 2010

STUDENT'S DECLARATION

I hereby declare that the work in this project is my own except for quotations and summaries which have been duly acknowledged. The project has not been accepted for any degree and is not concurrently submitted for award of other degree.

Signature
Name: MOHAMAD SHAFFAWI BIN ZAINON
ID Number: MA07033
Date: 6th DECEMBER 2010

Dedicated to my father, Zainon b. Ismail, my beloved mother, Che Sham bt Ishak and all my family members.

ACKNOWLEDGEMENTS

ABSTRACT

This thesis presented about the fatigue life of the material, which is focus on aluminium alloy. There are some important analysis needs to be done including stress analysis, and also fatigue analysis. People might prefer predict the fatigue life of aluminium alloy using experimental approach. But in this thesis, it comes out with different ways, by using software. The software used is MSC PATRAN with MSC NASTRAN as a solver and MSC Fatigue. The model is developed using the SOLIDWORKS. The results from initial analysis will be proceeding with second analysis which is fatigue simulation. Finally, the crack growth graph will be constructed. The effect of stress ranges of aluminium alloys on fatigue crack growth rate was simulated using the Compact Tension specimen as a model. The Fatigue Crack Growth curve, *da/dn* as a function of stress intensity factor, ΔK was plotted in order to analyze the crack growth properties of aluminium alloys. It has been done using MSC FATIGUE software. 4 different stress ranges were selected in range (4-10) kN in order to investigate the effect of stress range on crack growth rates. The model were simulated by means of Mode I loading in constant temperature and frequency. The constant value of **C** and gradient, **m** according to Modified Paris Law equation, are 1.2E-10 and 4.06 respectively. The life cycle graph (S-N curve) of aluminium alloy under this simulation will be compared to the established life cycle graph. It was show that the aluminium alloys have endurance limit of 95MPa.

ABSTRAK

Tesis ini membincangkan mengenai jangka hayat sesuatu bahan terhadap fenomena kelesuan bahan, yang memberi fokus kepada aloi aluminium. Terdapat beberapa analisis penting yang akan dilaksanakan termasuk analisis tegasan dan juga simulasi kelesuan bahan. Kebanyakan individu lebih suka untuk melakukan analisis jangka hayat kelesuan aloi aluminium dengan melakukan eksperimen, tetapi untuk tesis ini, simulasi perisian akan dilakukan untuk mendapatkan graf kadar pertumbuhan retak bagi aloi aluminium. Perisian yang digunakan ialah MSC PATRAN sebagai medium simulasi awal dan MSC NASTRAN and MSC Fatigue sebagai medium simulasi akhir. Hasil daripada setiap analisis akan dikumpul untuk menghasilkan graf pertumbuhan retak. Kesan julat tegasan terhadap kadar pertumbuhan retak kelesuan bagi aloi aluminium telah disimulasi menggunakan spesimen Tegasan Padat (Compact Tension Specimen) sebagai model. Graf kadar pertumbuhan retak melawan keamatan teganan telah dihasilkan bertujuan untuk mengenalpasti sifat – sifat aloi aluminium. Ia telah dihasilkan melalui Perisian MSC Fatigue. 4 julat tegasan yang berbeza telah dipilih untuk simulasi ini, iaitu di dalam julat (4-10) kN dalam mengenalpasti kesan julat tekanan terhadap kadar pertumbuhan retak. Model ini disimulasi menggunakan Mod 1 dan pada suhu dan frekuensi yang tetap. Berdasarkan persamaan Paris yang diubah (Modified Paris Law), nilai pintasan paksi Y ialah 1.2E-10 dan nilai kecerunan ialah4.06 Graf jangka hayat telah dihasilkan dan ia menunjukkan nilai batas ketahanan aloi aluminium ialah 47MPa.

TABLE OF CONTENTS

CHAPTER 5   **CONCLUSION AND RECOMMENDATIONS**

LIST OF TABLES

LIST OF FIGURES

LIST OF SYMBOLS

Δ	Differential
σ	Stress
N	Number of Cycles
Al_2O_3	Aluminium Oxide
Al-Si	Aluminium Silicon

LIST OF ABBREVIATIONS

AA   Aluminium Alloy

ANSI   American National Standard Institute

CT   Compact Tension

DIN   Deutsch Institute for Normung (German Standardization Institute)

FCC   Face centred cubic

FEA   Finite Element Analysis

FEM   Finite Element Method

IACS   International Annealed Copper Standard

IADS   International Alloy Designation System

IR   Infra Red

ISO   International Standard Organization

UV   Ultra Violet

CHAPTER 1

INTRODUCTION

1.1   INTRODUCTION

The analysis of failures often reveals various weaknesses contributing to an insufficient fatigue resistance of a structure. This will be illustrated by a case history. A structure should be designed and produced in such a way that undesirable fatigue failures do not occur. Apparently there is a challenge which will be referred to as designing against failure. Various design options can be adopted to ensure satisfactory fatigue properties with respect to sufficient life, safety and economy, which are related to different structural concepts, more careful detail design, less fatigue sensitive material, improved material surface treatments, alternative types of joints, lower design stress level.

Fatigue is failure under a repeated or varying load, never reaching a high enough level to cause failure in a single application. The fatigue process embraces two basic domains of cyclic stressing or straining, differing distinctly in character. In each domain, failure occurs by different physical mechanisms:

(a) Low-cycle fatigue—where significant plastic straining occurs. Low-cycle fatigue involves large cycles with significant amounts of plastic deformation and relatively short life. The analytical procedure used to address strain-controlled fatigue is commonly referred to as the Strain-Life, Crack-Initiation, or Critical Location approach.

(b) High-cycle fatigue—where stresses and strains are largely confined to the elastic region. High-cycle fatigue is associated with low loads and long life. The Stress-

Life (S-N) or Total Life method is widely used for high-cycle fatigue applications. While low-cycle fatigue is typically associated with fatigue life between 10 to 100,000 cycles, high-cycle fatigue is associated with life greater than 100,000 cycles.

Fatigue analysis refers to one of three methodologies: local strain or strain life, commonly referred to as the crack initiation method, which is concerned only with crack initiation (E-N, or sigma nominal); stress life, commonly referred to as total life (S-N, or nominal stress); and crack growth or damage tolerance analysis, which is concerned with the number of cycles until fracture.

The three methods used to predict life include total life (S-N), crack initiation (E-N), and crack growth. S-N analysis is relatively straightforward, being based on the nominal stress-life method using rain flow cycle counting and Palmgren-Miner linear damage summation. A range of analysis parameters may be selected, including Goodman or Gerber mean stress corrections, confidence parameters, manufacturing details (surface finish), and material heat treatments.

1.2   PROJECT BACKGROUND

The analysis of crack growth is very important and its need to widely known by engineer and designer. This analysis comes to the priority because there are so many accidents occur nowadays. The accident such as aircraft accidents, building collapse, and bridge collapse is mostly caused by material failure. This failure includes two types, which is overloading and fatigue failure. This analysis will focus on fatigue failure or cyclic loading. The fatigue life is usually split into crack initiation period and a crack growth period.

The initiation period is supposed to include some micro crack growth, but the fatigue cracks are still too small to be visible by the unaided eye. In the second period, the crack is growing until complete failure. It is technically significant to consider the crack initiation and crack growth periods separately because several practical conditions have a large influence in the crack initiation period, but a limited influence or no

influence at all on the crack growth period. In the analysis, the stress range values, ΔK threshold and ΔK critical will be determined in fatigue crack growth rate curve. The analysis will using Finite Elements Analysis (FEA) and stress strain analysis. It will also using a mode 1 under axial loading, and for the stress analysis, it will use a MSC PATRAN and MSC NASTRAN as pre-processor, solver, and post-processor. The final result will display in stress elements, strain elements, displacement element and also force elements. For the model in software stimulation, compact tension (CT) model is the best model to use since we apply the axial loading. There are parameters include in this analysis to determine the ΔK from fatigue crack growth rate curve, like cyclic loading, temperature, weight, and environment conditions. All this parameters need be constant.

1.3   PROBLEM STATEMENT

Predicting fatigue life is a critical aspect of the design cycle because virtually every product manufactured will wear out or break down. The critical issues are whether the product/component/assembly will reach its expected life, and if damaged, whether the product/component/assembly will remain safely in service until the damage can be discovered and repaired. And as with most simulation analysis, the earlier fatigue analysis is deployed in the product development process, the more benefits will be realized, including safety and economic.

For example, fatigue analysis early in the design phase can locate areas that are likely to succumb to fatigue quickly, minimizing expensive and unnecessary prototypes and tests. Due to this problem, common products manufactured are using non-suitable material. Aluminium alloys have a good characteristic in order to prevent or minimize the crack such as what happened to steel. So, analysis will be conduct on aluminium alloy to approve that aluminium alloy is better. The analysis will using Finite Elements Analysis (FEA) and stress strain analysis. The final result will display in stress elements, strain elements, displacement element and also force elements.

1.4   PROJECT OBJECTIVES

(i) To construct a curve of fatigue crack growth rate (differential crack length respect to number of load cycles to the range of stress intensity factor).

(ii) To determine the of stress intensity factor at threshold point and critical point.

(iii) To analyze and determine the S-N curve by numerical method using modified Paris Law equation.

1.5   SCOPES OF PROJECT

Scope of this project is limited to:

1. Investigate the effects of stress range on fatigue crack growth.
2. Identify the behavior of aluminum alloy under cyclic stress range under axial loading
3. Predict the total life of aluminum alloy based on fracture mechanics equation, from fatigue crack growth rate curve.
4. Analyze the model of Compact Tension (CT) in simulation using Finite Elements Analysis.

CHAPTER 2

LITERATURE REVIEW

2.1   INTRODUCTION

This final year project basically analyze on the fatigue behaviour of aluminium alloy under Mode 1 or axial loading. The topic needs to be discussed and conclude because each material has their limitations. This research also important as reference to anyone especially manufacturers while produce a part using metal. Fatigue is the progressive and localized structural damage that occurs when a material is subjected to cyclic loading. The nominal maximum stress values are less than the ultimate tensile stress limit, and may be below the yield stress limit of the material.

Fatigue occurs when a material is subjected to repeat loading and unloading. If the loads are above a certain threshold, microscopic cracks will begin to form at the surface. Eventually a crack will reach a critical size, and the structure will suddenly fracture. The shape of the structure will significantly affect the fatigue life; square holes or sharp corners will lead to elevated local stresses where fatigue cracks can initiate. Round holes and smooth transitions or fillets are therefore important to increase the fatigue strength of the structure.

2.2   FINITE ELEMENT ANALYSIS
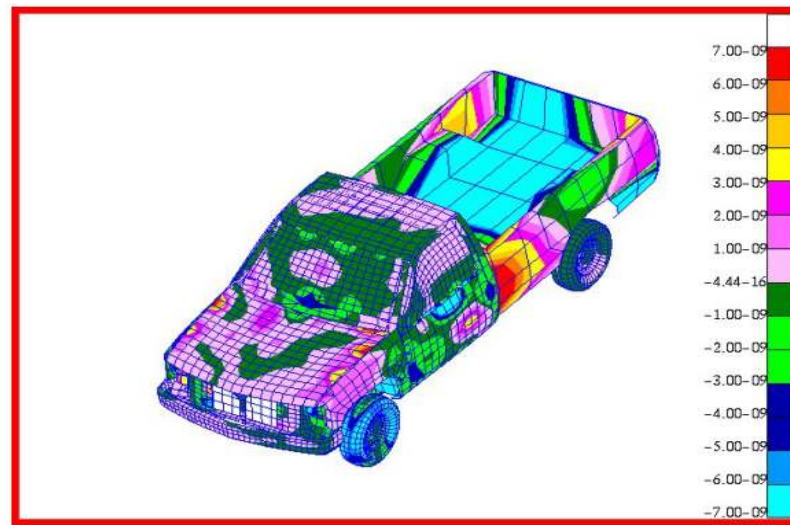
Figure 2.1: The example of finite element analysis on part.

Source: Christophe Pierre 2003

The boundary conditions applied to the mesh included a cyclically varying uniform traction with a minimum value and a maximum value applied on the surface for the axial loading analysis. To prevent rigid body movement, all nodes on the bottom surface of the mesh were fixed in the vertical (two-axis) direction. The nodes at the lower right hand corner were additionally fixed in the one-axis direction. This simulation model is actually a half part of the actual model. Smaller the component simulated, the result will be clearer and easy to analyze. The mesh was created with nodal pairs along the crack propagation path. The contact elements can also be used to prevent elements overlapping along the crack surface. During loading, the applied traction increased from minimum shear to maximum shear. Crack advance was executed with the loading held constant at maximum shear. The crack was grown by releasing all of the connector elements currently at the crack tip. The newly released connector elements were then replaced by contact elements. During the unloading cycle, the applied traction was returned to minimum shear. (Elwood 1992)

The finite element method (FEM) (its practical application often known as finite element analysis (FEA) is a numerical technique for finding approximate solutions of partial differential equations. The opening stress for each cycle was defined as the applied tensile stress on the uppermost elements of the aluminium alloy specimen when the crack first completely opened. The contact pressure for each crack surface node was monitored during the loading stage of each cycle. When all of the crack surface nodes in a particular calculation region (specimen surface or specimen interior) first experienced zero contact pressure, the applied tensile stress was the opening stress in the region. Although this is just a small angle disorientations, particles are more significant than bicrystal boundaries for fatigue crack growth as will be shown later in this paper when larger disorientations angles were employed. (Horstemeyer 2009)

2.3   SOFTWARE USED FOR MODEL SIMULATION

There is a lot of software available for Finite Element Analysis, such as ALGOR (FEMPRO), ANSYS, ABAQUS, and MSC PATRAN. All this software widely used nowadays, in order to analyze the part. In solving partial differential equations, the primary challenge is to create an equation that approximates the equation to be studied, but is numerically stable, meaning that errors in the input and intermediate calculations do not accumulate and cause the resulting output to be meaningless. There are many ways of doing this, all with advantages and disadvantages. The Finite Element Method is a good choice for solving partial differential equations over complicated domains.

The most suitable software used in this Finite Element Analysis is MSC PATRAN, because the Linear Static results will be proceed with Fatigue Analysis. The final analysis will determine the objective of this Final Year Project, which is generated Crack Growth from simulation under axial loading. From this graph, Life Cycle graph of metal also can be calculated, using a modified Paris Law or fracture mechanic equation. This simulation also will produce a data analysis of Safety Factor in order to prove that load applied is acceptable.
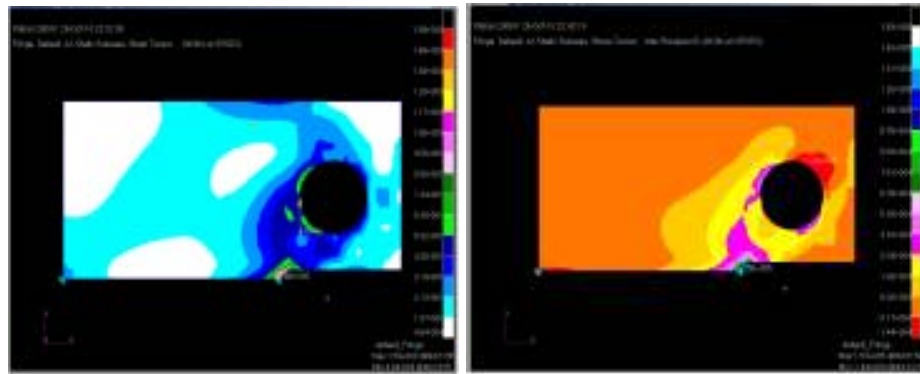
Figure 2.2: Example of MSC PATRAN analysis.

Source: www.mscsoftware.com/Solutions/Applications/Default.aspx

2.3.1 Crack Growth Graph from Database

Using MSC PATRAN as software in simulation is beneficial because it already provide user with database results. There are so many database graph that we can produced, include the Crack Growth graph. Even though we can use the database graph for results, it is not accurate according to the simulation. The final data must be different from analysis, especially *C* Value (Y-axis intercept) and *m* Value (Gradient of the straight line). In conclusion, the database results only act as references, and the Crack Growth Graph must be generated from the simulation and fatigue analysis.

Delta K Apparent Plot

AISI_4340: Ratio 0.2   Environment: air
C: 1.3E-11 m: 2.8 Kc: 61   D0: 3.9 D1: 2   Rc: 0.88

Delta K Apparent Plot

AISI_4340: Ratio 0.6   Environment: air
C: 1.3E-11 m: 2.8 Kc: 61   D0: 3.9 D1: 2   Rc: 0.88
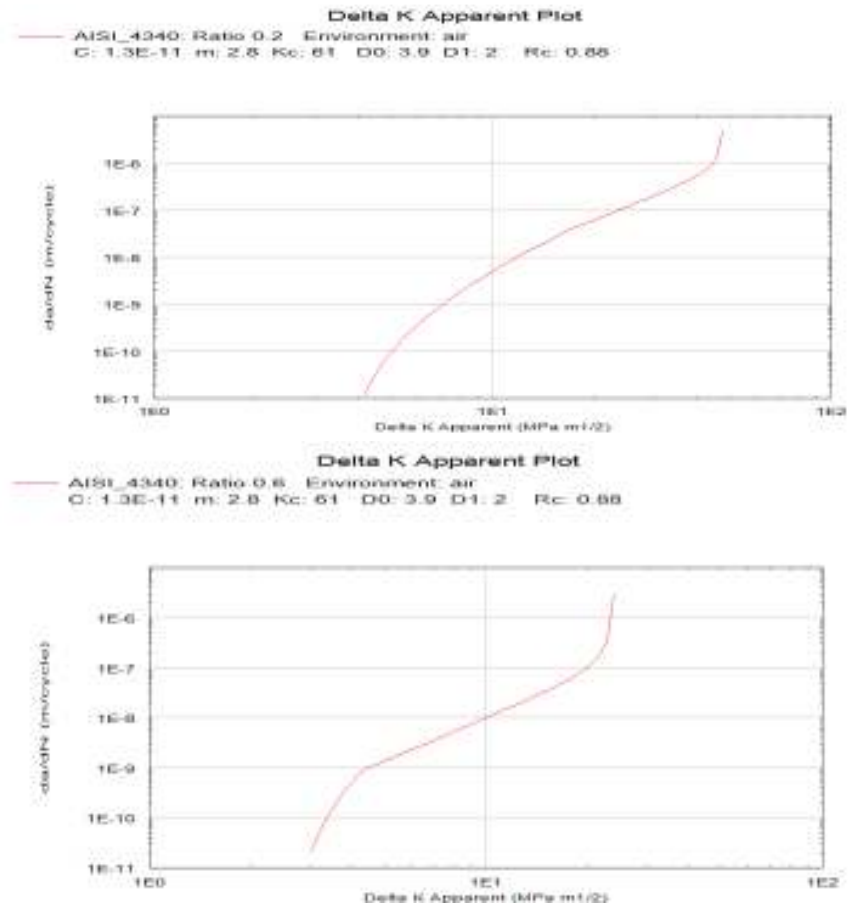
Figure 2.3: The crack growth graph get from the database for different stress
ratio values.

Source: www.mscsoftware.com/Products/CAE-Tools/MSC-Fatigue.aspx

The Stress Ratio, R that inserted manually is different which is 0.2 and 0.6.
Although the Stress Ratio is different but *C* Value (Y-axis intercept) and *m* Value
(gradient of straight line) is constant. The data can't be used to create S-N Curve
manually from Paris Law Equation.

2.4 MATERIAL SELECTION

The research material selection must be accurate and beneficial in future. As well as this Final Year Project use Aluminium Alloy (AA 1060), it's properly fulfill the requirement of needed data to produce a product. This type of material is widely used especially in producing automotive parts and other tooling parts.

2.4.1 History of Aluminium

The earliest citation given in the Oxford English Dictionary for any word used as a name for this element is aluminium, which British chemist and inventor Humphry Davy employed in 1808 for the metal he was trying to isolate electrolytically from the mineral *alumina*. The citation is from the journal *Philosophical Transactions of the Royal Society of London*: "Had I been so fortunate as to have obtained more certain evidences on this subject, and to have procured the metallic substances I was in search of, I should have proposed for them the names of silicium, alumium, zirconium, and glucium.

Aluminum is the third most abundant element of the Earth's crust, behind that of oxygen and silicon. Of the metallic elements, it is the most abundant, 7.3% by mass of the total crust. Due to Aluminum's high affinity to bind with oxygen, it is not found in naturally occurring in its elemental state, but only in combined forms such as oxides or silicates. The metal originally obtained its name from the Latin word for alum, *alumen*. Finally, in 1807, Sir Humphrey Davy proposed that this still unknown metal be referred to as *aluminum.* This was then altered further to that of *aluminium* so to agree with the "ium" spelling that ended most of the elements. This is the spelling that is generally used throughout the world. That is, until the American Chemical Society in 1925 officially reverted the spelling back to *aluminum*, which is how it is normally spelled in the United States. (Kaufman 2004)

2.4.2   Aluminium Alloy

For the pure aluminium, it is a soft, durable, lightweight, malleable metal with appearance ranging from silvery to dull grey, depending on the surface roughness. Aluminium is nonmagnetic and none sparking. It is also insoluble in alcohol, though it can be soluble in water in certain forms. The yield strength of pure aluminium is 7–11 MPa, while aluminium alloys have yield strengths ranging from 200 MPa to 600 MPa. Aluminium has about one-third the densit and stiffness of steel. It is ductile, and easily machined, cast, drawn and extruded. Corrosion resistance can be excellent due to a thin surface layer of aluminium oxide that forms when the metal is exposed to air, effectively preventing further oxidation. The strongest aluminium alloys are less corrosion resistant due to galvanic reactions with alloyed copper. This corrosion resistance is also often greatly reduced when many aqueous salts are present, particularly in the presence of dissimilar metals. (Ishihara 2001)

Aluminium atoms are arranged in a face-centred cubic (fcc) structure. Aluminium has stacking-fault energy of approximately 200 mJ/m^2. Aluminium is one of the few metals that retain full silvery reflectance in finely powdered form, making it an important component of silver paints. Aluminium mirror finish has the highest reflectance of any metal in the 200–400 nm (UV) and the 3,000–10,000 nm (far IR) regions; in the 400–700 nm visible range it is slightly outperformed by tin and silver and in the 700–3000 (near IR) by silver, gold, and copper. Aluminium is a good thermal and electrical conductor, having 62% the conductivity of copper.

Aluminium is capable of being a superconductor, with a superconducting critical temperature of 1.2 Kelvins and a critical magnetic field of about 100 gauss (10 milliteslas). It is a strongly reactive metal that forms a high-energy chemical bond with oxygen. Compared to most other metals, it is difficult to extract from ore, such as bauxite, due to the energy required to reduce aluminium oxide (Al_2O_3). For example, direct reduction with carbon, as is used to produce iron, is not chemically possible, since aluminium is a stronger reducing agent than carbon. Aluminium is the most widely used non-ferrous metal. Global production of aluminium in 2005 was 31.9 million tonnes.

It exceeded that of any other metal except iron (837.5 million tonnes). Forecast for 2012 is 42–45 million tons, driven by rising Chinese output. Relatively pure aluminium is encountered only when corrosion resistance and/or workability is more important than strength or hardness. A thin layer of aluminium can be deposited onto a flat surface by physical vapour deposition or (very infrequently) chemical vapour deposition or other chemical means to form optical coatings and mirrors. When so deposited, a fresh, pure aluminium film serves as a good reflector (approximately 92%) of visible light and an excellent reflector (as much as 98%) of medium and far infrared radiation.

Table 2.1 Mechanical properties of pure aluminium.

Mechanical Properties	Values
Youngs Modulus	70 GPa (in alloys)
Ductility & Malleability	High
Hardness	420 MPa
Density	2700 kg / m³
Melting Point	660.32 °C
Boiling Point	2519 °C
Electrical Resistivity	2.65×10^{-8} Ωm
Reflectivity	71% (unpolished) 97% (polished)

Source: http: http://sam.davyson.com/as/physics/aluminium/site/properties.html

Aluminium alloys are alloys in which aluminium is the predominant metal. Typical alloying elements are copper, zinc, manganese, silicon, and magnesium. There are two principal classifications, namely casting alloys and wrought alloys, both of which are further subdivided into the categories heat-treatable and non-heat-treatable. About 85% of aluminium is used for wrought products, for example rolled plate, foils and extrusions. Cast aluminium alloys yield cost effective products due to the low melting point, although they generally have lower tensile strengths than wrought alloys. The most important cast aluminium alloy system is Al-Si, where the high levels of silicon (4-13%) contribute to give good casting characteristics. Aluminium alloys are widely used in engineering structures and components where light weight or corrosion resistance is required.

Aluminium alloy surfaces will keep their apparent shine in a dry environment due to the formation of a clear, protective oxide layer. Aluminium alloys with a wide range of properties are used in engineering structures. Alloy systems are classified by a number system (ANSI) or by names indicating their main alloying constituents (DIN and ISO). Selecting the right alloy for a given application entails considerations of strength, ductility, formability, workability, weld ability and corrosion resistance to name a few. A brief historical overview of alloys and manufacturing technologies is given in Ref. Aluminium is used extensively in modern aircraft due to its high strength to weight ratio. (Allison 1991)

2.4.3   Aluminum Alloy in Applications

Conductors in either the 1000 or 6000 series alloys are sensible technical alternatives to copper for all electrical conductors, even in domestic wiring. A very large proportion of overhead, high voltage, power lines utilize aluminium rather than copper as the conductor on weight grounds. The relatively low strength of these grades requires that they be reinforced by including a galvanized or aluminium coated high tensile steel wire in each strand.

Aluminium alloys have a conductivity averaging 62% of the International Annealed Copper Standard (IACS) but, because of its density, it can carry more than twice as much as electricity as an equivalent weight of copper. Aluminium and its alloys have been the prime material of construction for the aircraft industry throughout most of its history. Even today, when titanium and composites are growing in use, 70% of commercial civil aircraft airframes are made from aluminium alloys, and without aluminium civil aviation would not be economically viable. The combination of acceptable cost, low component mass (derived from its low density), appropriate mechanical properties, structural integrity and ease of fabrication are also attractive in other areas of transport. There are now very many examples of its use in commercial vehicles, rail cars both passenger and freight, marine hulls and superstructures and military vehicles.

Volume car production now includes aluminium as engine castings, wheels, radiators and increasingly as body parts. For general production the 5000 and 6000 series alloys provide adequate strength combined with good corrosion resistance, high toughness and ease of welding. In aircraft the very strong 2000, 7000 and 8000 series alloys are preferred, and in military vehicles the weldable 7000 series alloys can provide ballistic properties to match steel armour. (Hudak 1974)

The addition of scandium to aluminium creates nanoscale Al_3Sc precipitates which limit the excessive grain growth that occurs in the heat-affected zone of welded aluminium components. Scandium is also a potent grain refiner in cast aluminium alloys, and atom for atom, the most potent strengthened in aluminium, both as a result of grain refinement and precipitation strengthening. However, titanium alloys, which are stronger but heavier, are cheaper and much more widely used.

The main application of metallic scandium by weight is in aluminium-scandium alloys for minor aerospace industry components. These alloys contain between 0.1% and 0.5% (by weight) of scandium. They were used in the Russian military aircraft MIG 21 and MIG 29. Some items of sports equipment, which rely on high performance materials, have been made with scandium-aluminium alloys, including baseball bats, lacrosse sticks, as well as bicycle frames and components. U.S. gun maker Smith & Wesson produces revolvers with frames composed of scandium alloy and cylinders of titanium. (Schultz 2005)

2.5 Fatigues in Metal

Fatigue is the progressive and localized structural damage that occurs when a material is subjected to cyclic loading. The nominal maximum stress values are less than the ultimate tensile stress limit, and may be below the yield stress limit of the material. (Tianwen 2007)

Fatigue occurs when a material is subjected to repeat loading and unloading. If the loads are above a certain threshold, microscopic cracks will begin to form at the surface. Eventually a crack will reach a critical size, and the structure will suddenly

fracture. The shape of the structure will significantly affect the fatigue life; square holes or sharp corners will lead to elevated local stresses where fatigue cracks can initiate. Round holes and smooth transitions or fillets are therefore important to increase the fatigue strength of the structure. In metals and alloys, the process starts with dislocation movements, eventually forming persistent slip bands that nucleate short cracks.

Fatigue is a stochastic process, often showing considerable scatter even in controlled environments, and the greater the applied stress range, the shorter the life. Fatigue life scatter tends to increase for longer fatigue lives, and damage is cumulative. (Caddel 1976)

2.5.1 Factors That Affect the Fatigue Life

i. Cyclic stress state: Depending on the complexity of the geometry and the loading, one or more properties of the stress state need to be considered, such as stress amplitude, mean stress, biaxiality, in-phase or out-of-phase shear stress, and load sequence.

ii. Geometry: Notches and variation in cross section throughout a part lead to stress concentrations where fatigue cracks initiate.

iii. Surface quality: Surface roughness cause microscopic stress concentrations that lower the fatigue strength. Compressive residual stresses can be introduced in the surface by e.g. shot peening to increase fatigue life. Such techniques for producing surface stress are often referred to as peening, whatever the mechanism used to produce the stress.

iv. Material Type: Fatigue life, as well as the behavior during cyclic loading, varies widely for different materials, e.g. composites and polymers differ markedly from metals.

v.   Residual stresses: Welding, cutting, casting, and other manufacturing processes involving heat or deformation can produce high levels of tensile residual stress, which decreases the fatigue strength.

vi.   Size and distribution of internal defects: Casting defects such as gas porosity, non-metallic inclusions and shrinkage voids can significantly reduce fatigue strength.

vii. Direction of loading: For non-isotropic materials, fatigue strength depends on the direction of the principal stress.

viii. Grain size: For most metals, smaller grains yield longer fatigue lives, however, the presence of surface defects or scratches will have a greater influence than in a coarse grained alloy.

ix.   Environment: Environmental conditions can cause erosion, corrosion, which all affect fatigue life. Corrosion fatigue is a problem encountered in many aggressive environments.

x.   Temperature: Extreme high or low temperatures can decrease fatigue strength.

2.6   FRACTURE MECHANICS EQUATION

Fracture mechanics is the field of mechanics concerned with the study of the propagation of cracks in materials. It uses methods of analytical solid mechanics to calculate the driving force on a crack and those of experimental solid mechanics to characterize the material's resistance to fracture. In modern materials science, fracture mechanics is an important tool in improving the mechanical performance of materials and components. It applies the physics of stress and strain, in particular the theories of elasticity and plasticity, to the microscopic crystallographic defects found in real materials in order to predict the macroscopic mechanical failure of bodies.
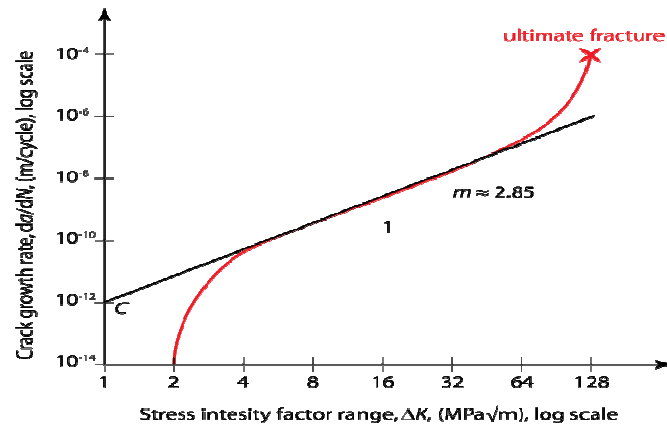
Figure 2.4: The example of crack growth graph and uses of Paris Law Equation.

Source: Allison 1991

The Paris-Erdogan law (more commonly known as Paris' law) relates the stress intensity factor range to sub-critical crack growth under a fatigue stress regime. As such, it is the most popular Fatigue Crack Growth model used in materials science and fracture mechanics. The basic formula reads

$$\frac{da}{dN} = C\Delta k^m$$

(2.1)

Where a is the crack length and N is the number of load cycles. Thus, the term on the left side, known as the Crack Growth Rate denotes the crack length growth per increasing number of load cycles. On the right hand side, C and m are material constants, and ΔK is the range of the stress intensity factor.

2.6.1 Modified Paris Law Equation

Since the Paris Law is only for the Paris region or region 2, it must be modified in order to calculate the bigger region. Paris region only consider for the straight line, while there still a life cycle and crack propagation even in other region.

$$\frac{da}{dN} = C(\Delta K^m - \Delta K_{th}^m)$$

(2.2)

The modified Paris Law equation will determined the crack propagation value of the model. Where *a* is the crack length and *N* is the number of load cycles. Thus, the term on the left side, known as the Crack Growth Rate denotes the crack length growth per increasing number of load cycles. On the right hand side, *C* and *m* are material constants, and ΔK is the range of the stress intensity factor. This equation use stress intensity at critical point, and also at threshold point where the crack is starting to propagate.

2.7 LIFE CYCLE GRAPH (S-N CURVE)

The S-N method is used in a variety of situations, including long life fatigue problems where there is little plasticity, and for components where crack initiation or crack growth modelling is not appropriate, such as non-ferrous materials, composites, welds, and plastics. The example of S-N Curve is shown below in figure below.

Figure 2.5: Example of S-N Curve.

Source: Caddel 1976

CHAPTER 3

METHODOLOGY

3.1   INTRODUCTION

This chapter is focused on the methodology process which is the sets of methods to analyze fatigue crack growth. The model that been implement are need to specify certain criteria to achieve project objectives. The information in the literature review is interpreted to select the suitable load, material, mesh density, stress ratio and type of specimen. The model needs to be specified in PATRAN software model. The steps that involve in analyzing the model are stated. Lastly, stress analysis is done by NASTRAN.

The three methods use different techniques with different degrees of accuracy. Note that in theory this equation is true, but in practice it seldom works when the three methods are applied to the same problem. In reality, it's unusual to utilize the three methods on the same problem, because different industries favour different design philosophies, which drive the analysis methods.

3.2 FLOW CHART

For overall of the project, there a flow charts to show the general flow of this project.
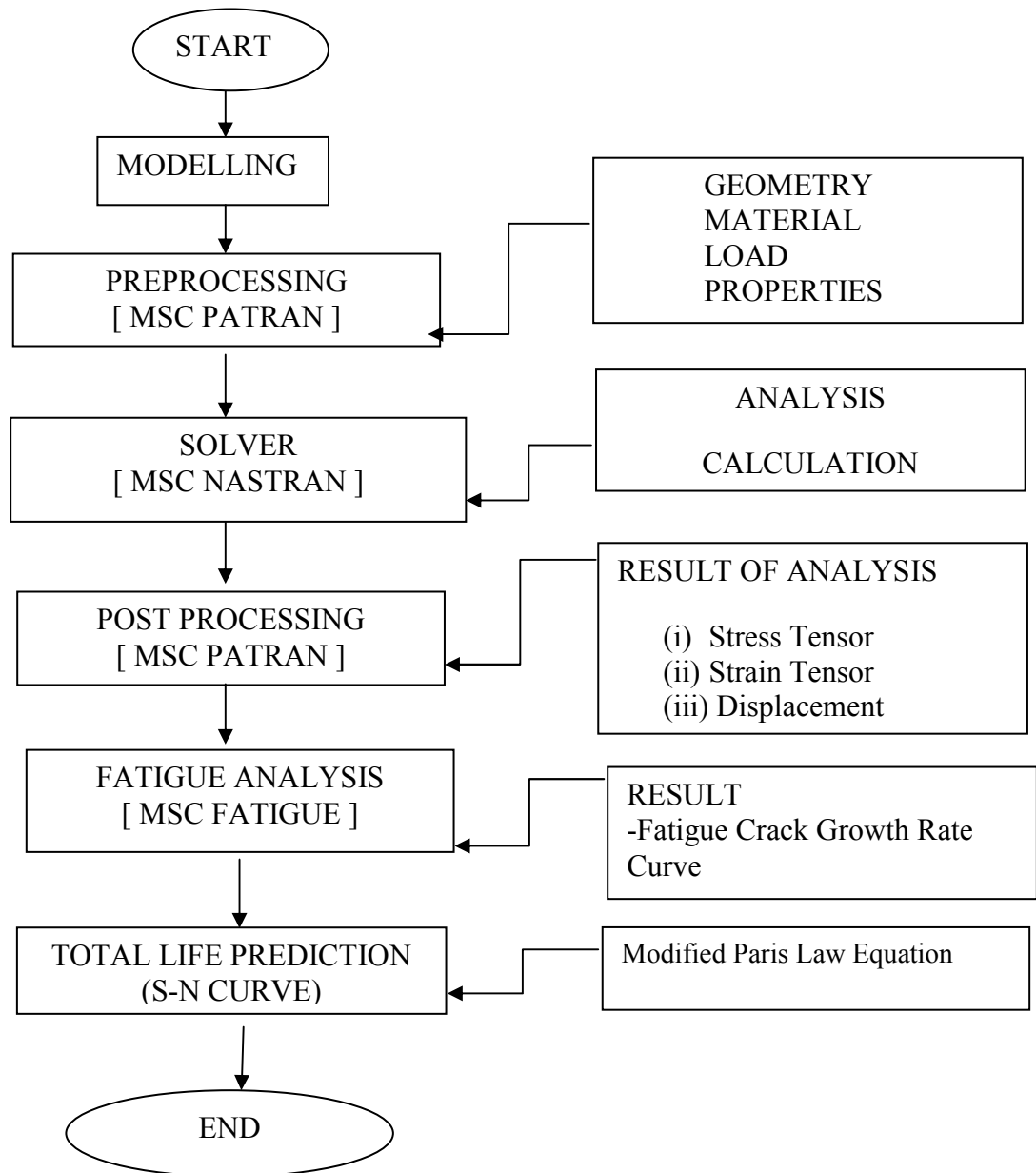
Figure 3.1: Flow chart of the project

To achieve the objectives of this project, a methodology has been constructed. The methodology flow chart is purposed to give guidelines and directions to successfully accomplish the main goal of this project. The following is the summary methodology flow chart
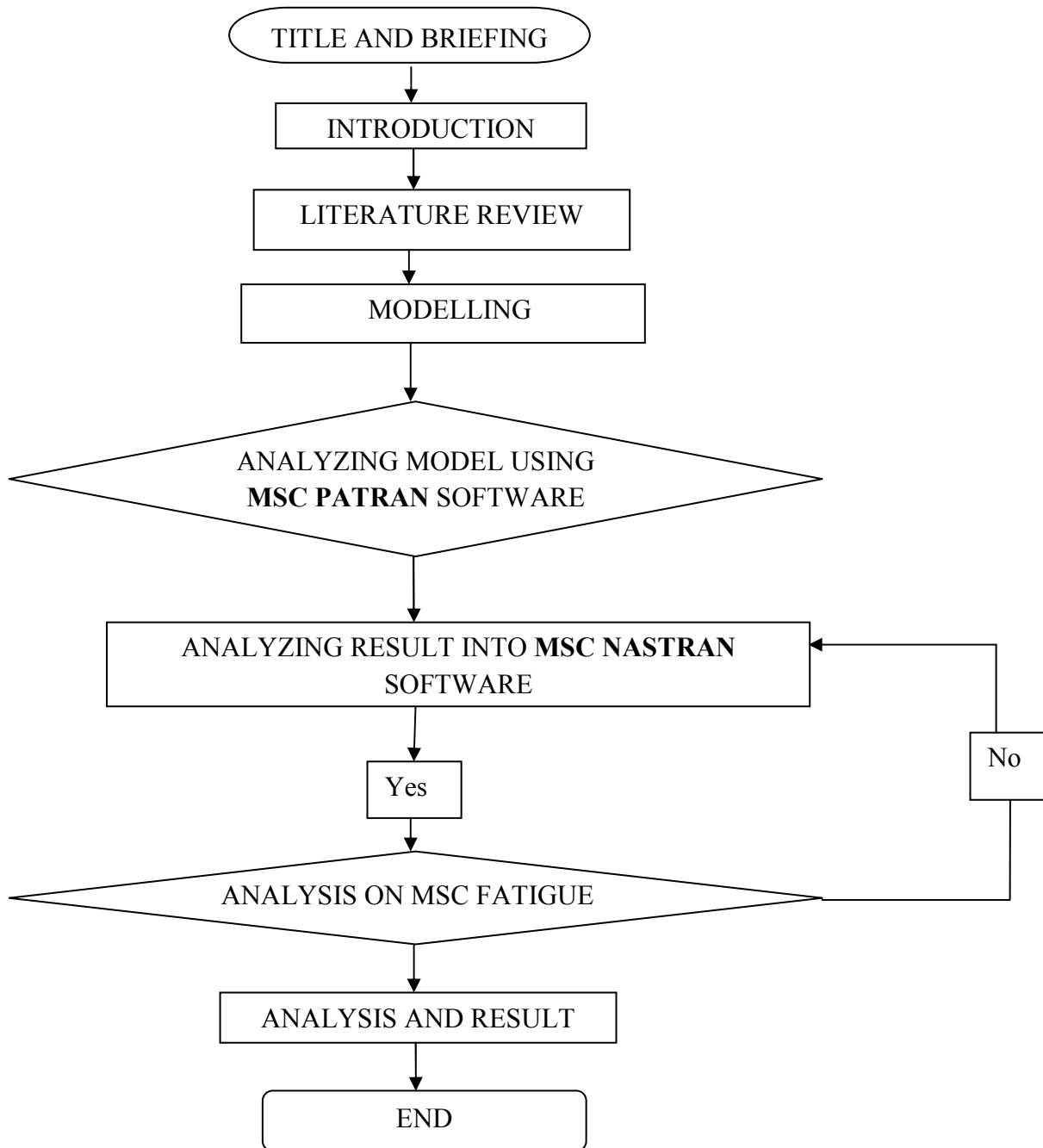
Figure 3.2: Methodology flow chart

3.3   MATERIAL

Using metal material such as steel or stainless steel is common chosen material in fatigue life prediction analysis. When we come out with different material which is aluminium alloy, it is beneficial analysis because there can be a comparison between the two material, depend on the part requested. Aluminium alloy AA1060 is widely used, and this is main reason for the material selection.

3.3.1   Aluminium Alloy

Aluminium alloys are alloys in which aluminium is the predominant metal. Typical alloying elements are copper, zinc, manganese, silicon, and magnesium. There are two principal classifications, namely cast alloys and wrought alloys, both of which are further subdivided into the categories heat-treatable and non-heat-treatable. About 85% of aluminium is used for wrought products, for example rolled plate, foils and extrusions.

Cast aluminium alloys yield cost effective products due to the low melting point, although they generally have lower tensile strengths than wrought alloys. The most important cast aluminium alloy system is Al-Si, where the high levels of silicon (4-13%) contribute to give good casting characteristics.

The properties of aluminium alloy used are stated in the table below

Table 3.1 Mechanical properties of aluminium alloy AA 1060

Properties	Values
Density	2.7×1000 kg/m³
Poisson's Ratio	0.33
Elastic Modulus	70 – 80 GPa
Yield Strength	76 MPa
Shear Strength	55 MPa
Tensile Strength	83 MPa

Source: http://www.efunda.com/materials/alloys

3.4   MODELLING

There need to be modelling in this simulation in order to define geometry, properties, type of load, direction of load, and meshing process. Modelling process need to be accurate according to the international specification of Compact Tension specimen.

3.4.1   Modelling Method

To run the Linear Static analysis in MSC PATRAN, we can use both methods to get the analysis result, which is initial drawing in SOLIDWORKS before transfer, or sketch the model using MSC PATRAN geometry function. Better way is create a model in SOLIDWORKS, because it is easier and compatible in MSC PATRAN in term of Parasolid (.xt) format.

3.4.2 Modelling Using Solid Works
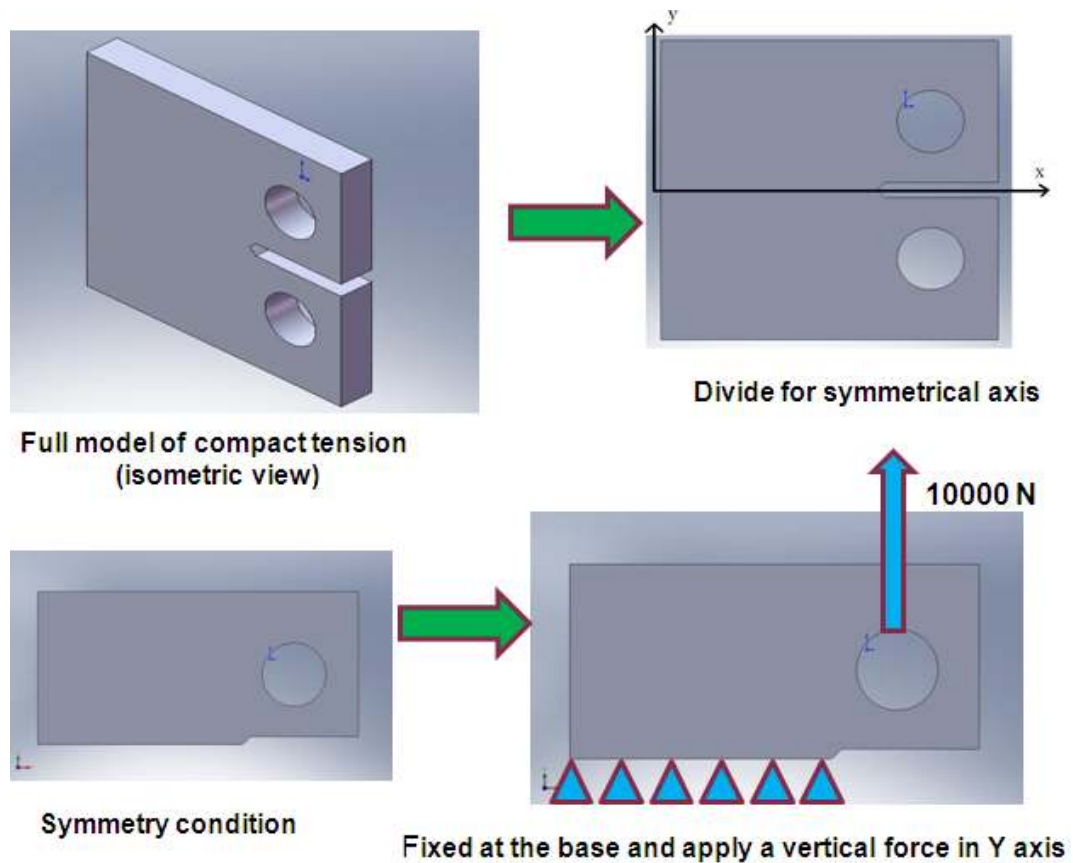
Figure 3.3: Modelling using SOLIDWORKS

3.5 MESHING

Meshing process is very important in order to complete the element analysis and produce the accurate results. The most suitable meshing need to analyze based on the size, and also ability of the processor or desktop.

3.5.1 Type of Meshing

Compact Tension specimen required a suitable meshing for the analysis, because the stress and strain result from MSC NASTRAN solver will be proceed to next step. If the mesh types are not suitable, the fatigue analysis will behave some problems and this

will damage the results. The chosen meshing type is tetrahedral, because this types of mesh fully symmetrical the Compact Tension specimen.

3.5.2 Meshing Efficiency

There are 6 size of mesh tried in this simulation. It is necessary to run all the 6 different mesh because we need to choose the most suitable mesh for simulation, and also to have a precise and accurate result. Mostly people will prefer a smallest size of mesh in simulation in order to have most accurate results, but we need to consider the ability of hardware (desktop) used. In fact, smaller mesh will take longer time to analyze and show final result. To make the analysis is not burden the desktop, this simulation use the second smallest mesh size, which is 0.04. Before choosing the most suitable size, the simulation also uses other size, and based on desktop efficiency, the smallest mesh which is 0.02 is not suitable. Otherwise, bigger mesh then 0.04 is not compatible with the requested results of analysis. The results of displacement tensor, strain and stress tensor are not really accurate due to meshing inefficiency.
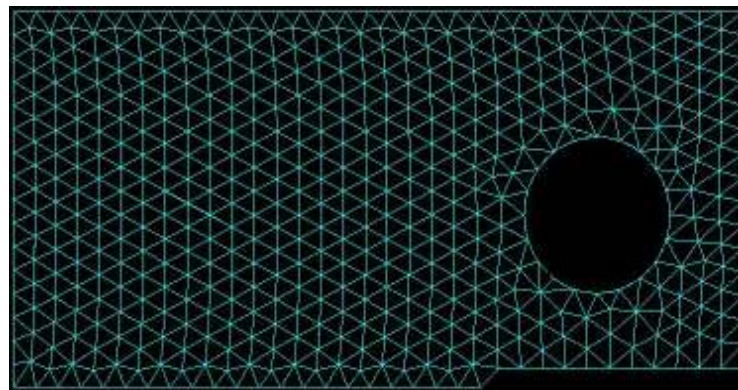
Figure 3.4: The mesh used in simulation after meshing efficiency consideration.

3.6   TYPE OF SIMULATION APPLIED LOADING

Basically, 3 type of apply loading available in fatigue life prediction. It is Mode 1 (Axial loading), Mode 2 (X-axis Shear loading) and the last one is Mode 3 (Horizontal Shear loading). This analysis uses Mode 1 because the type of force exerted

on specimen in widely happen. The force or load apply in axial form and model are seems to be pulled from above and below repeatedly. In fatigue life prediction, the load will keep on applied in simulation until the model achieves limitation of crack growth measurement.

In order to follow the scope of project, Stress Range R is constant. Even though there are variables of load applied in this stimulation, the maximum and minimum value need to be fixed. For all simulation, the Stress Range value is constant, which is 1.
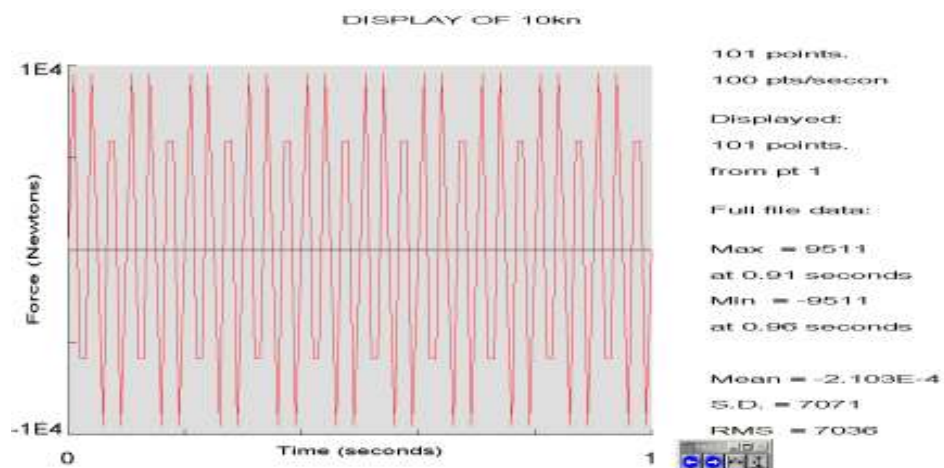
(a) Load = 10 kN
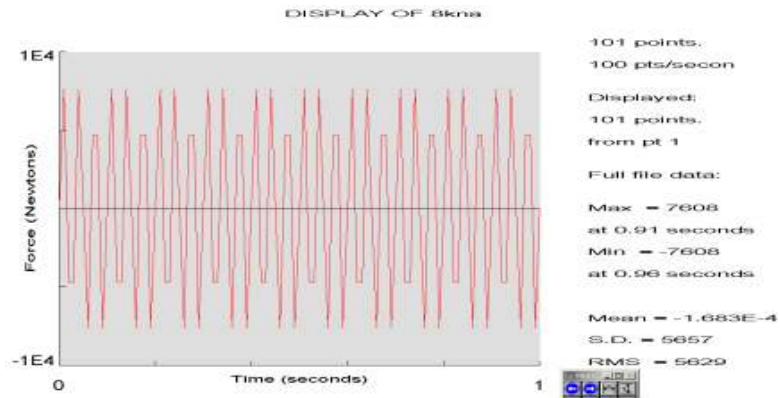
(b) Load = 8 kN
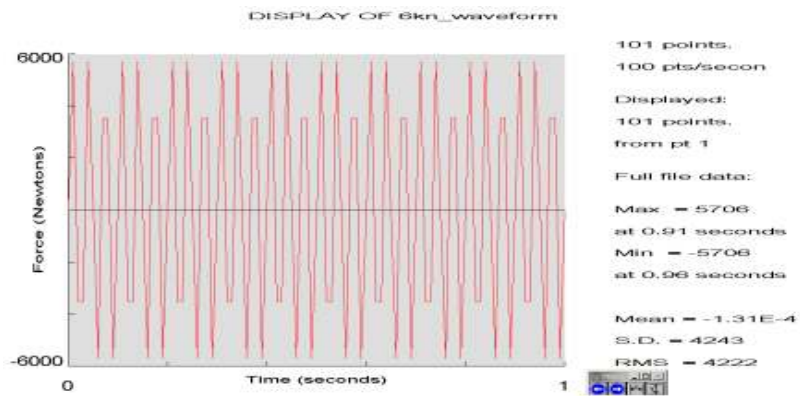
(c) Load = 6 kN
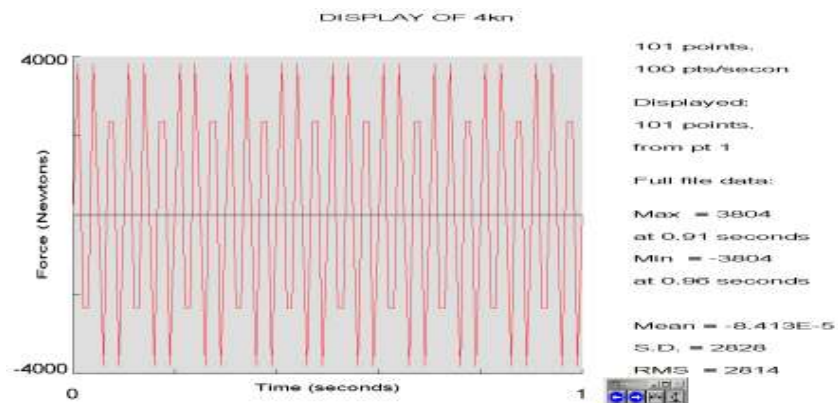
(d) Load = 4 kN

Figure 3.5: The waveform variable loads applied in the analysis.

CHAPTER 4

RESULT AND DISCUSSION

4.1   INTRODUCTION

This chapter discuss about the result obtained from the simulation by using the software and solver. The objective of this chapter is to determine the final result of the Compact Tension specimen and also its features. The data was collected, analyzed and graphs are constructed. The final graph of crack growth is generated from the simulation, and these results are little bit different from the software database. After the crack growth graph is generated, the values will used in substitution of Paris's Law Equation. While using a fix stress range value, the calculated data from Paris's law Equation will be transform into life cycle graph (S-N Curve). Finally, there will be a comparison between establish Life Cycle graph and generated Life Cycle graph based on stimulation. If there are similarities, it will prove that this simulation using Compact Tension Specimen under Mode 1 is correctly done, and the Crack Growth graph is theoretically can be generated with manual simulation using MSC PATRAN software.

4.2 RESULT

4.2.1 Linear Static Analysis

Since the best mesh has validated, which is 0.04, the simulations precede to the next step of analysis. After using MSC NASTRAN solver, the simulations are showing impressive result if displacement, strain tensor, and also a stress tensor. This simulation is using variable loads that have been fixed since the previous analysis. The purpose is to produce a different stress range in results in analysis.

i.   Load = 10kN

(a)   Displacement
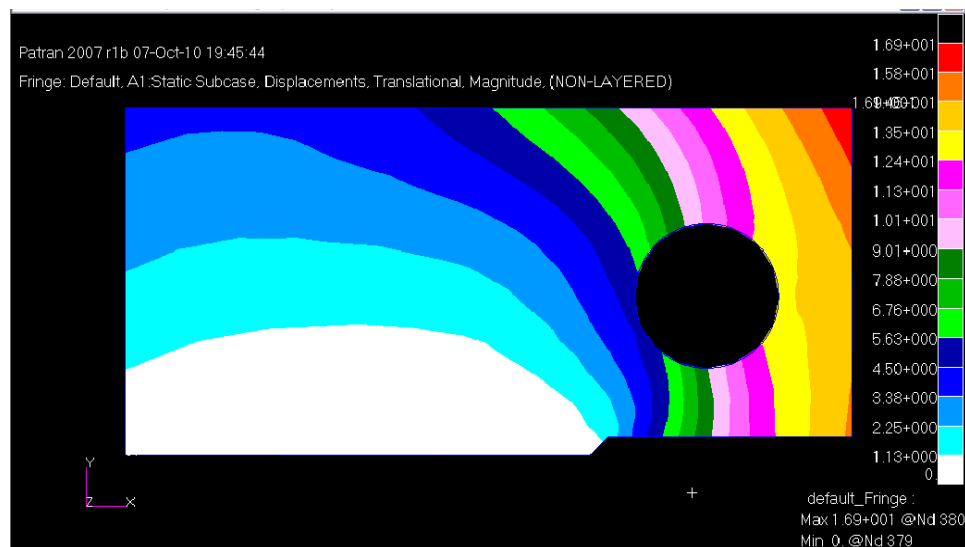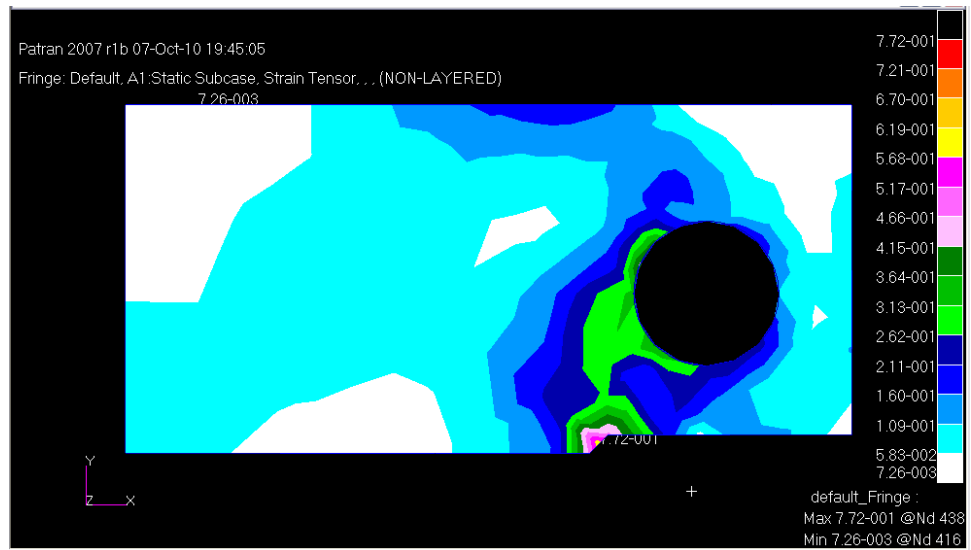
(b)   Strain Tensor
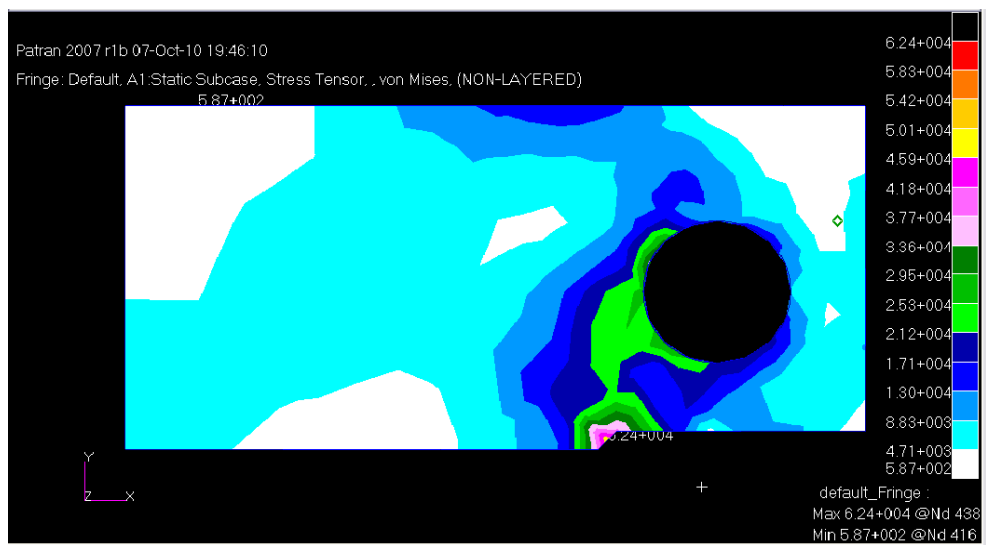
(c)   Stress Tensor

Figure 4.1: Linear static results for 10kN axial load simulation

ii. Load = 8kN

(a)   Displacement
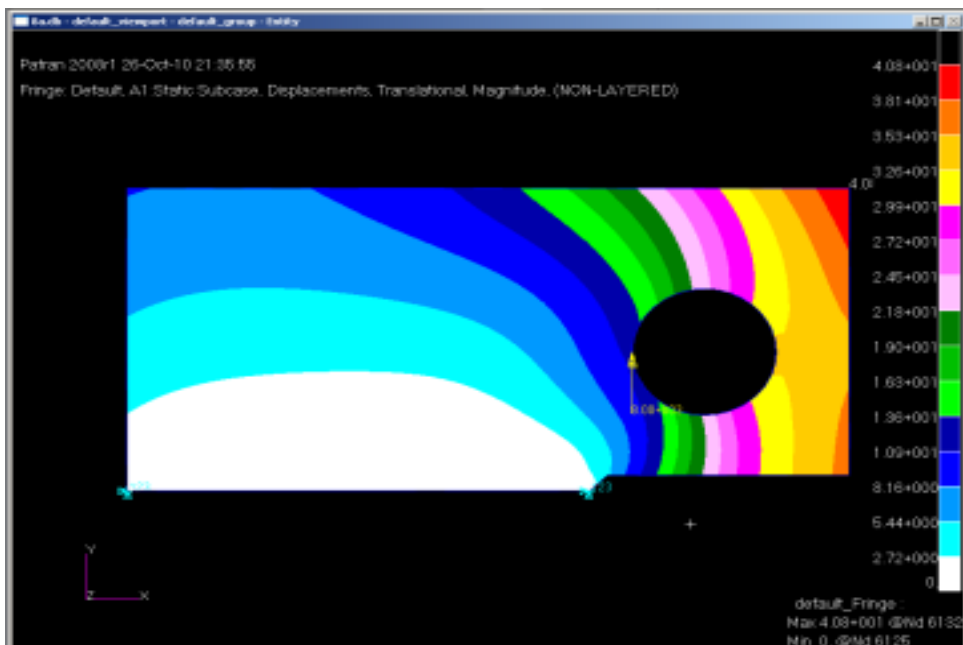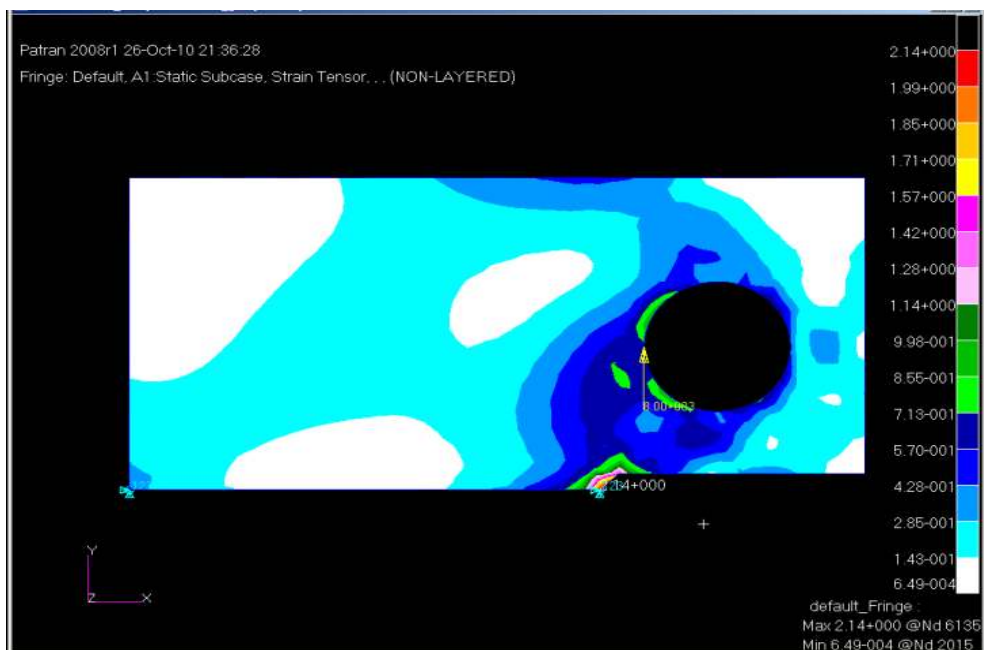
(b)   Strain Tensor
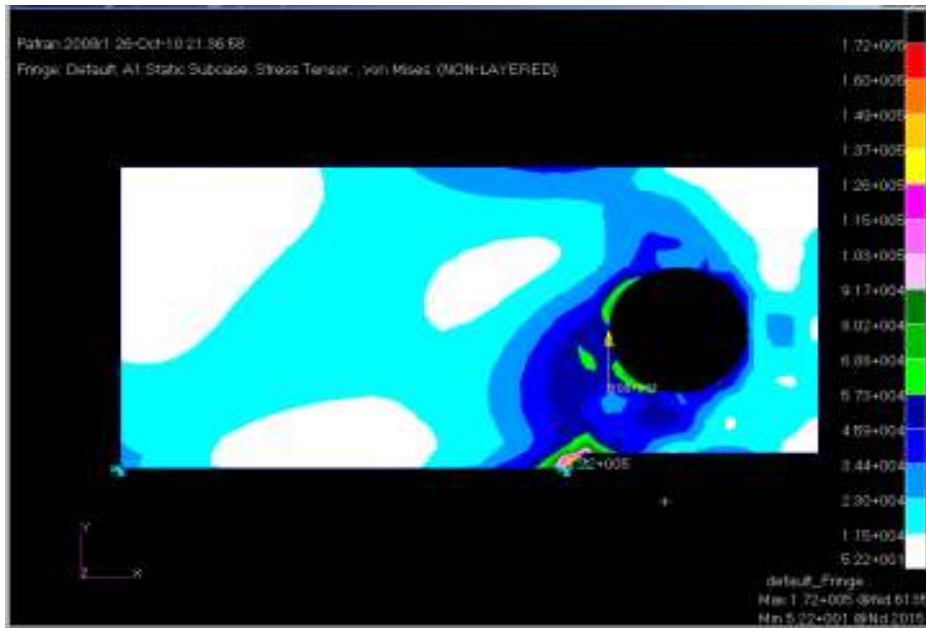
(c)   Stress Tensor

Figure 4.2: Linear static results for 8kN axial load simulation

iii. Load = 6kN

(a)   Displacement
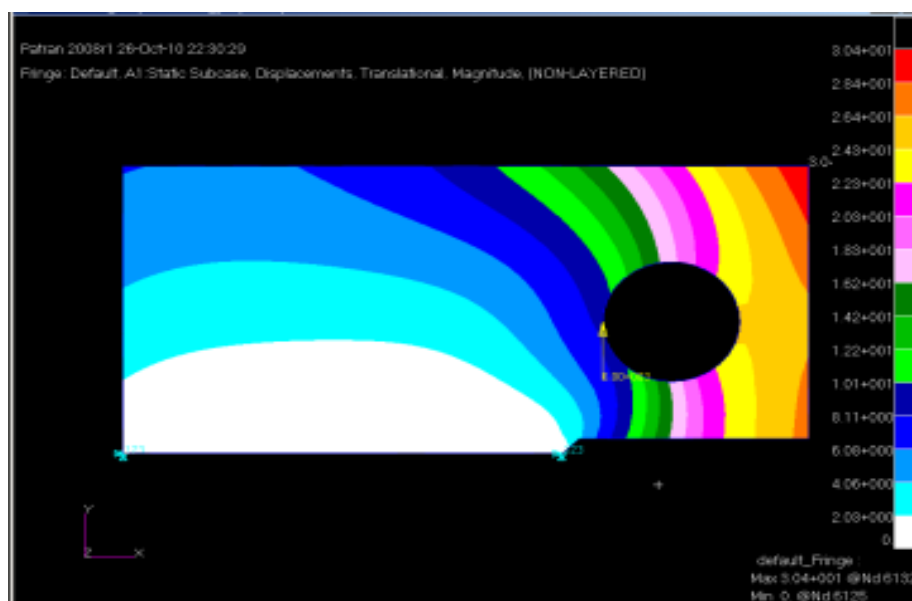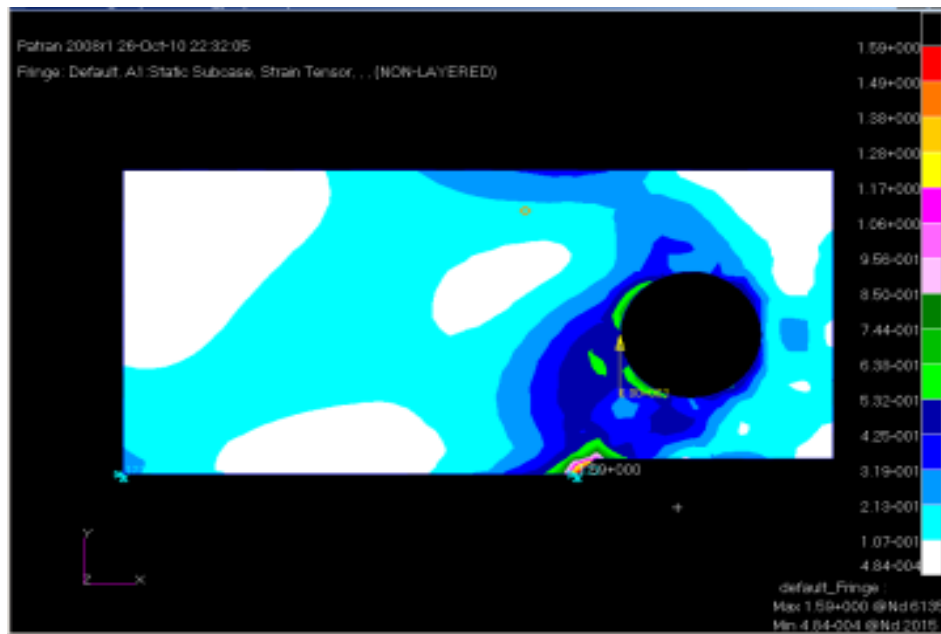
(b) Strain Tensor
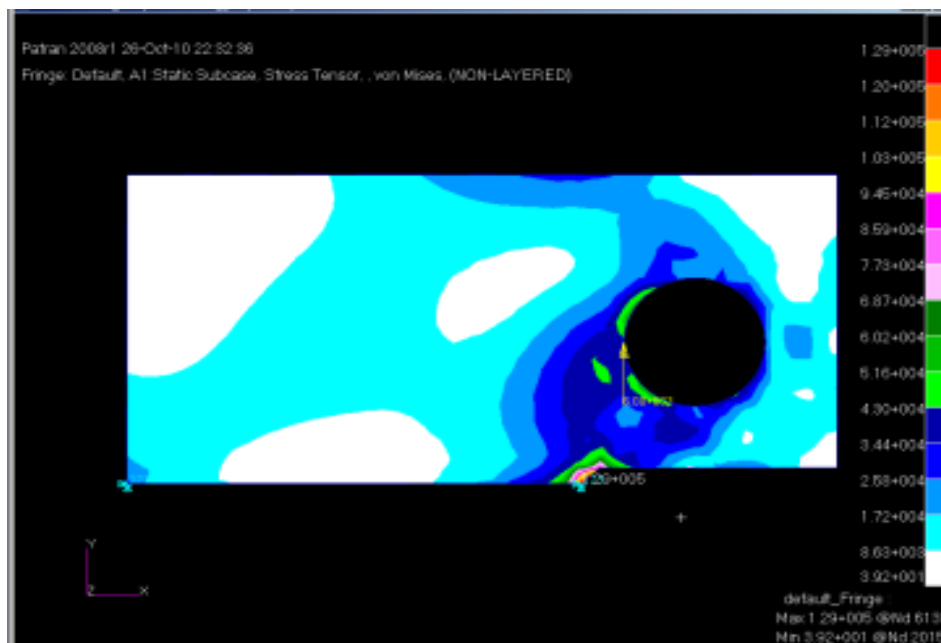
(c) Stress Tensor

Figure 4.3: Linear static results for 6kN axial load simulation

iv. Load = 4kN

    (a)   Displacement
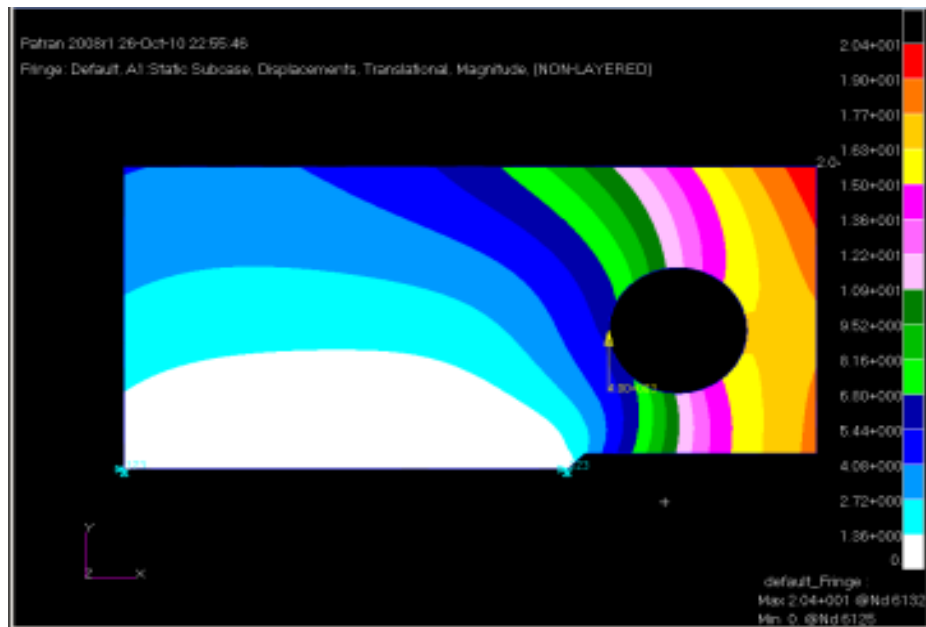
    (b)   Strain Tensor
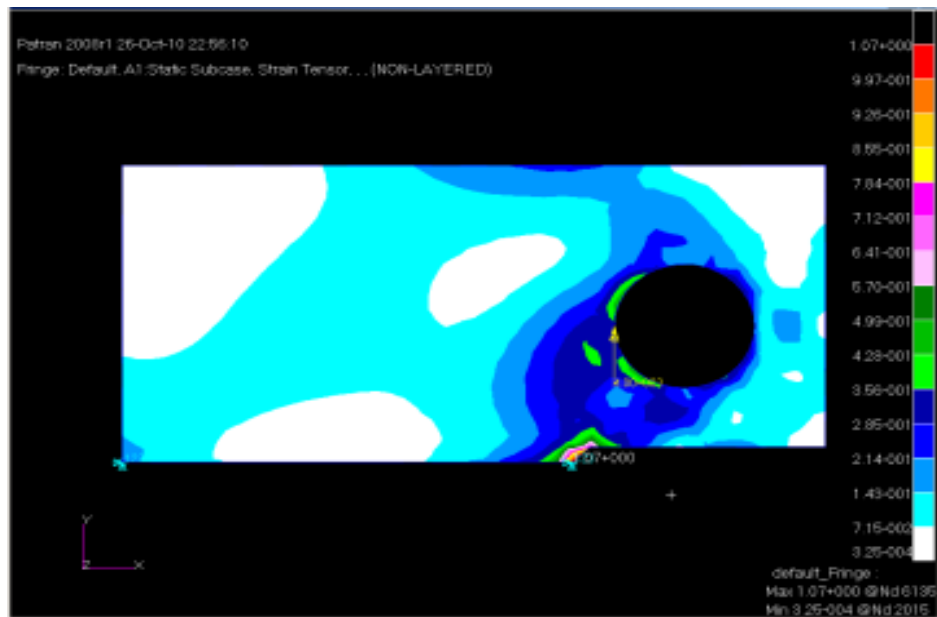
(c)   Stress Tensor
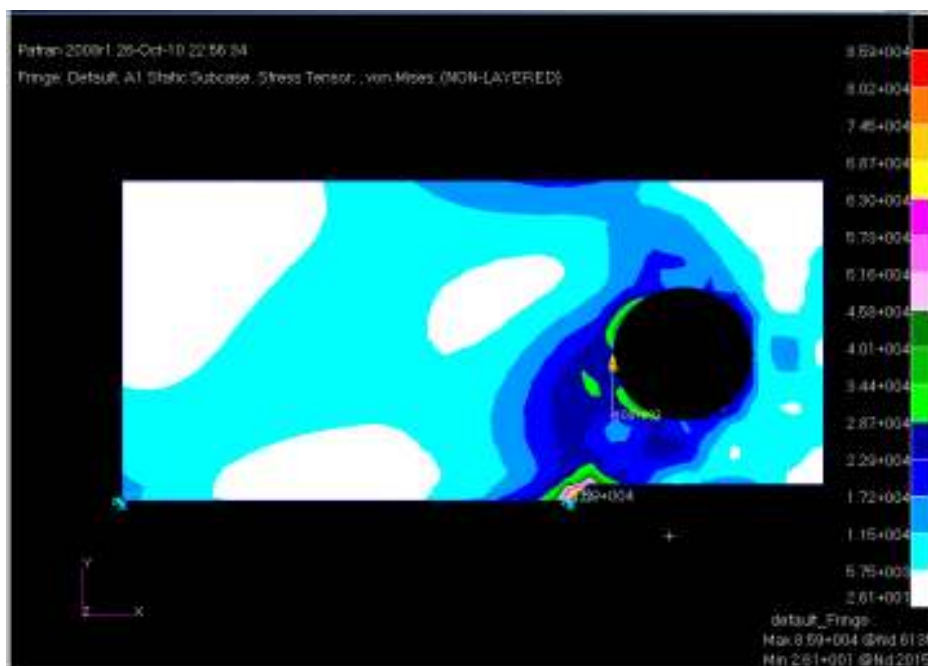
Figure 4.4: Linear static for 4kN axial load simulation

4.2.2   Fatigue Analysis Result

At present, the laws of material fracture under static loading in mode 1 are under active study. A lot of results of studies have been published concerning the laws of material fracture under cyclic mode 1. The aim of the present work is to study the laws of fatigue crack propagation threshold, Δk under cyclic loading. In propagation of fatigue cracks from the initiation to final fracture distinguished are a few stages, such as propagation of surface micro cracks in the plane of maximum shear stresses which is the process of a shear type. The propagation of the main crack coincides with the direction of the action of maximum normal stresses. Fracture occurs by tearing. The propagation of the main crack occurs in the plane of maximum shear stresses. Fracture occurs by shear.

(a)   Load = 10kN
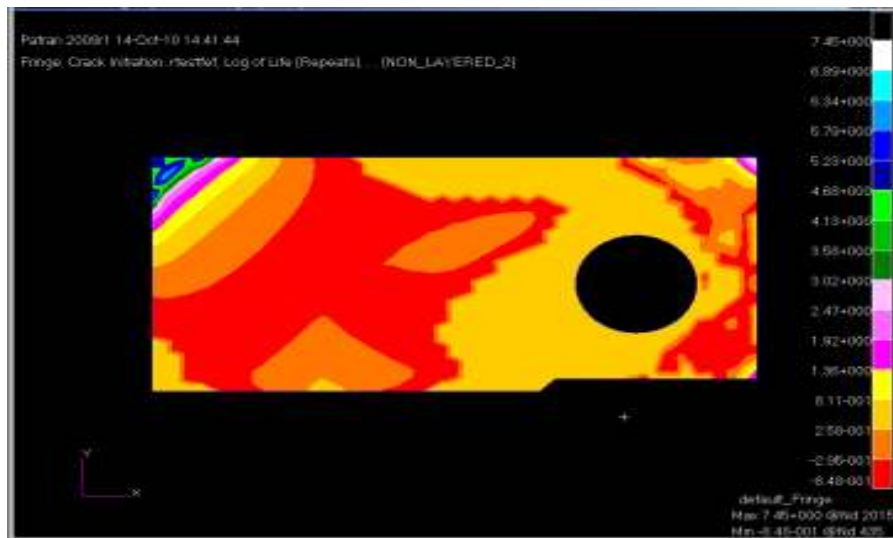
(b)   Load = 8kN
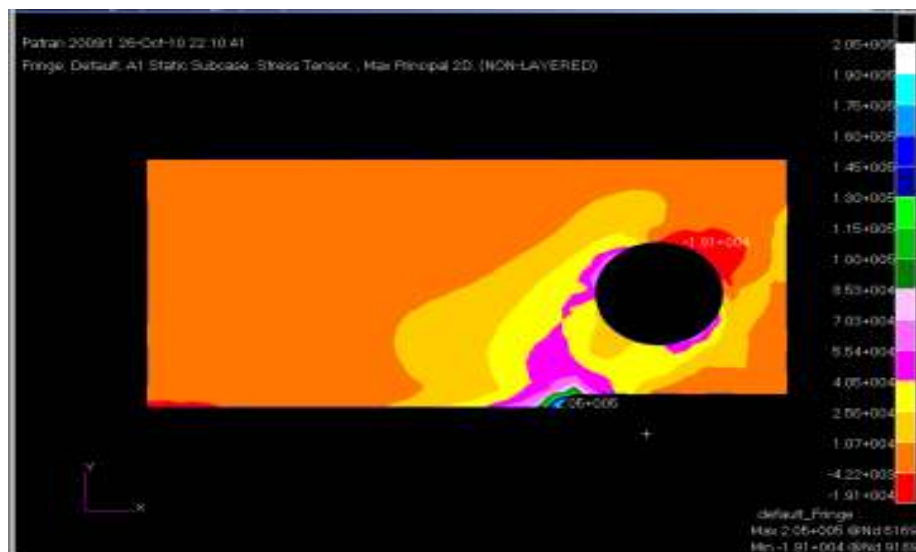
(c)   Load = 6kN
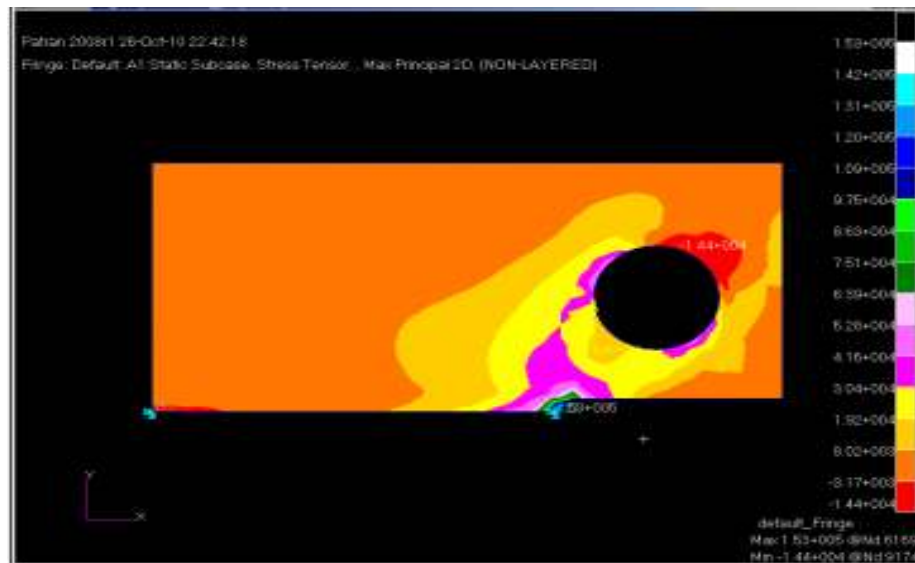
(d)   Load = 4kN
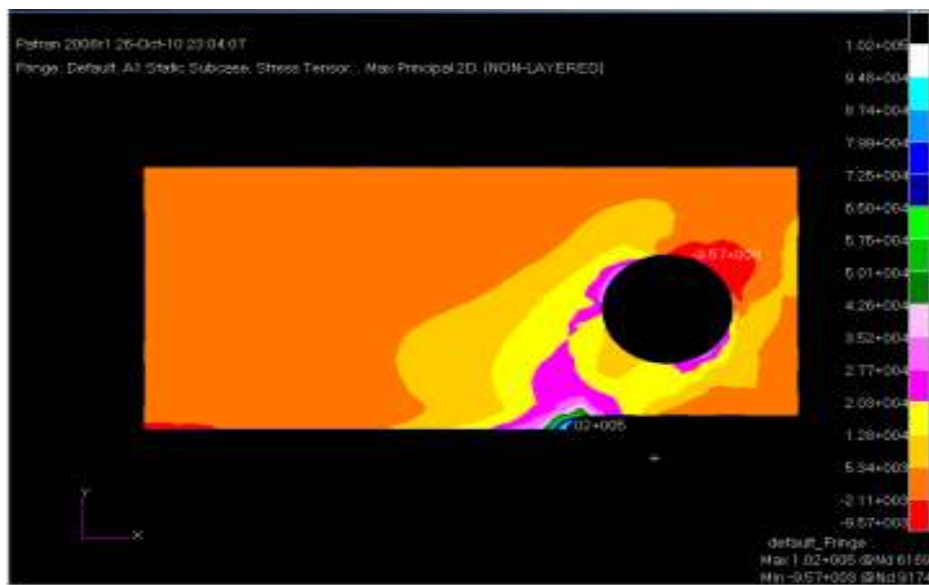
Figure 4.5: Fatigue analysis results for applied axial load

4.3   GRAPHICAL RESULTS

The analysis of the results presented shows that under mode 1 loading the resistance to Fatigue Crack Growth decreases as well as the values of Δk. It allows formulating the conditions of failure at the cyclic loading subject to the mechanism of crack propagation and values Δk. All the given simulation results prove that the presence of the shift component in the external loading increases the dander of failure and the role the influence the shift component to the characteristics of the cyclic crack resistance should not be neglected in the strength analysis. We do not give absolute significance to this prediction, but we would like to note its usefulness: the operating staff must understand what they have to prepare for, if the pipes from aluminium alloy.

4.3.1   Compliance Graph and Proportional Force

For the compliance graph, we can conclude the stimulation are going well, as the graph is seems to be proportional. The crack ratio is set to be limited from 0.2 till 0.8, and compliance value limited to 30 as in Y axis. Second graph show the proportional force applied in this stimulation. Even though overall load is repeated, but the graph show only in 1 cycle of loading, not in repeated loading. The value of the second graph is not really important, because our main objective is to apply a repeated loading with certain variable loads until the model having a crack in this stimulation. The final value of crack and number of cyclic loading obtained from the Crack Growth graph, with data served.
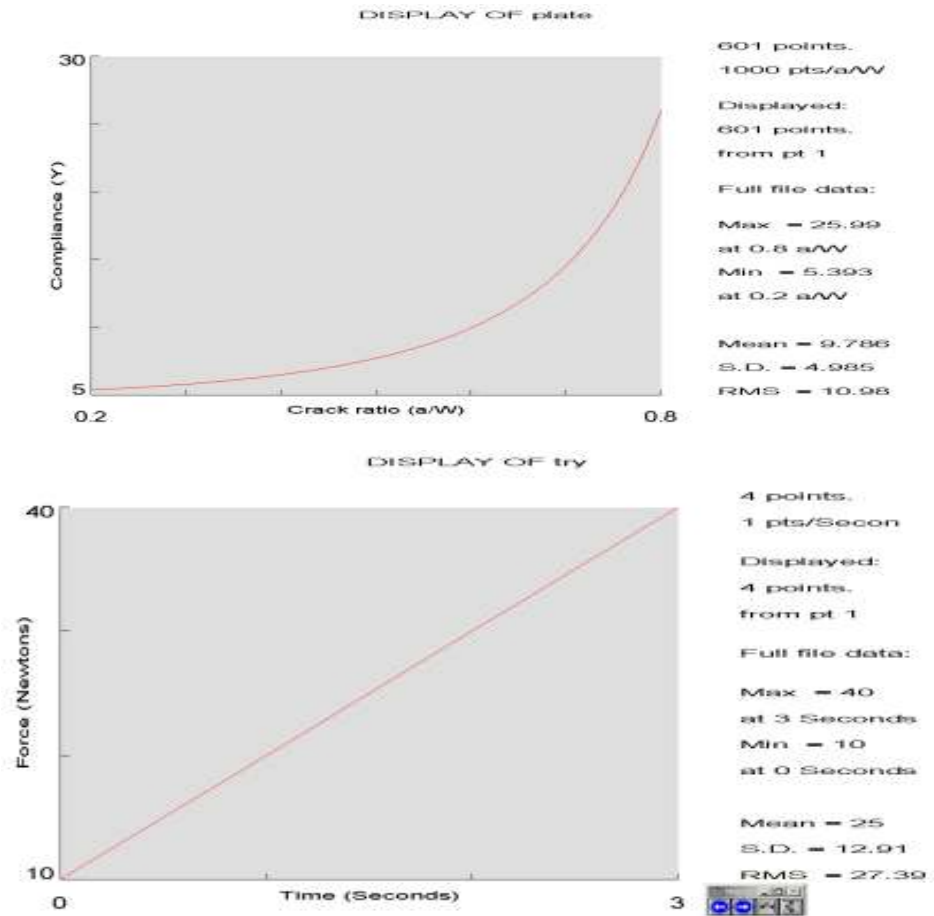
Figure 4.6: The compliance graph and force applied to the model in
simulation using MSC PATRAN

4.3.2 Comparing the Database Crack Growth Graph

In order to compare the result of simulation, there is database Crack Growth graph that can obtain easily. This database has multi choices of Stress Range, R that can be used, but the results are constant, in term of Y-axis intercept and gradient of the straight line of graph. Here are some examples of Crack Growth graph used R equal to 0.2, 0.4, and 0.6 produced from database result for the purpose of comparing.

Delta K Apparent Plot

AISI_4340: Ratio 0.6   Environment: air
C: 1.3E-11   m: 2.8   Kc: 61   D0: 3.9   D1: 2   Rc: 0.88
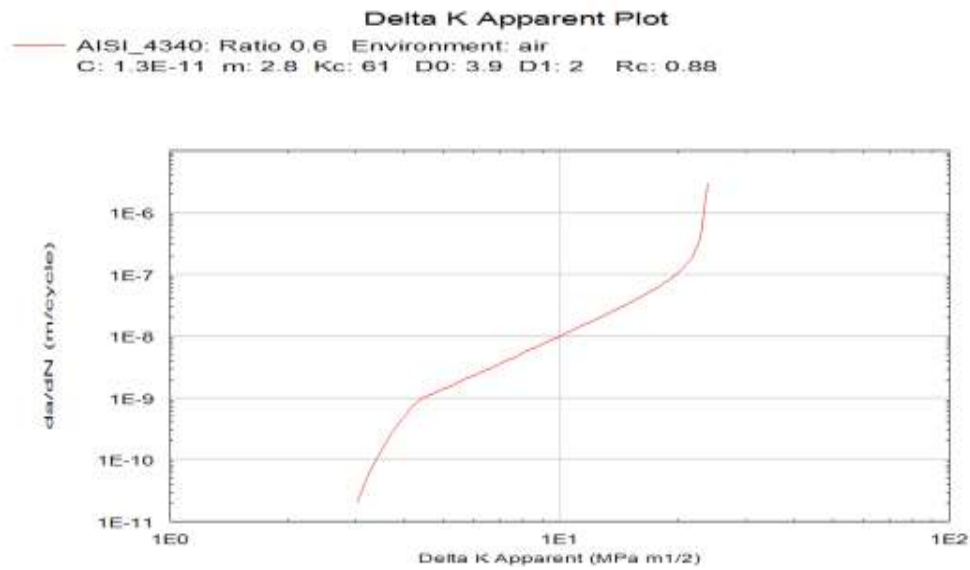
Figure 4.7: The crack Growth rate graph from the database in order to comparing with manual calculation in generating S-N curve.

4.3.3   Generated Crack Growth Graph

Simulation of aluminium alloy using MSC PATRAN with MSC FATIGUE as finalize analysis has produced a Crack Growth graph. This result is little bit different from database results in term of straight and smooth line construction. Even though in multi-point form, the gradient and Y-axis intercept still can be calculated. This generated values are approximately obey the limitation of the mode specification.
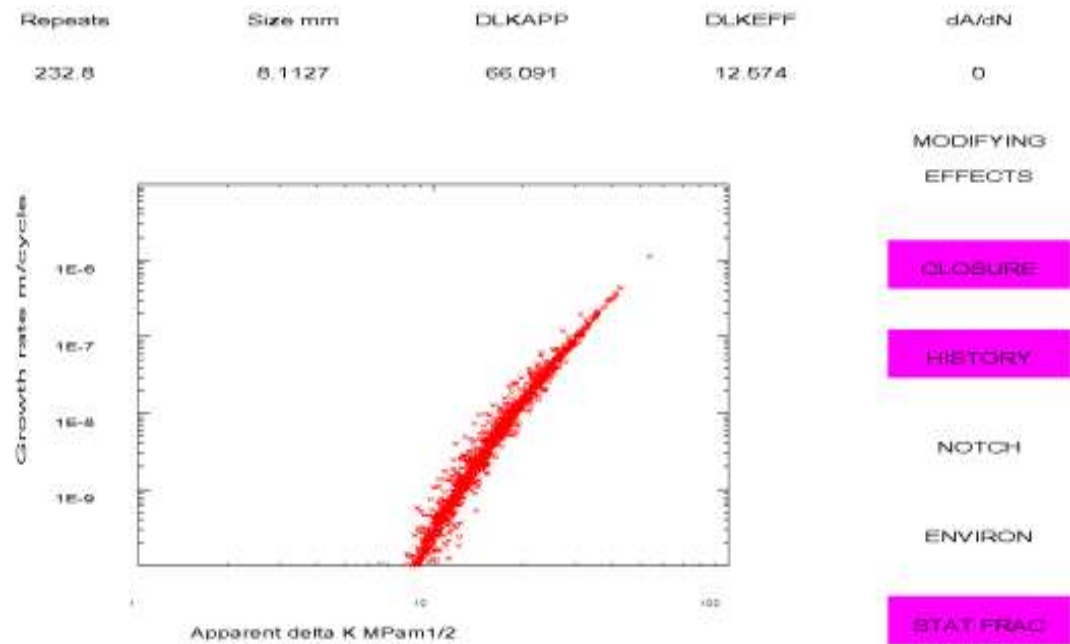
Figure 4.8: Generated crack growth curve from 10 kN simulation

The results are obeying the specification that inserted before the graph was plotted. Most important part is the crack size and cyclic time repeats. Both values will determine the accuracy of this simulation and whether this final result can be used for references or not. The figure below show the other crack growth generated from simulation, using 8kN load and 6kN. For the S-N curve prediction, only 10kN load will be chosen.
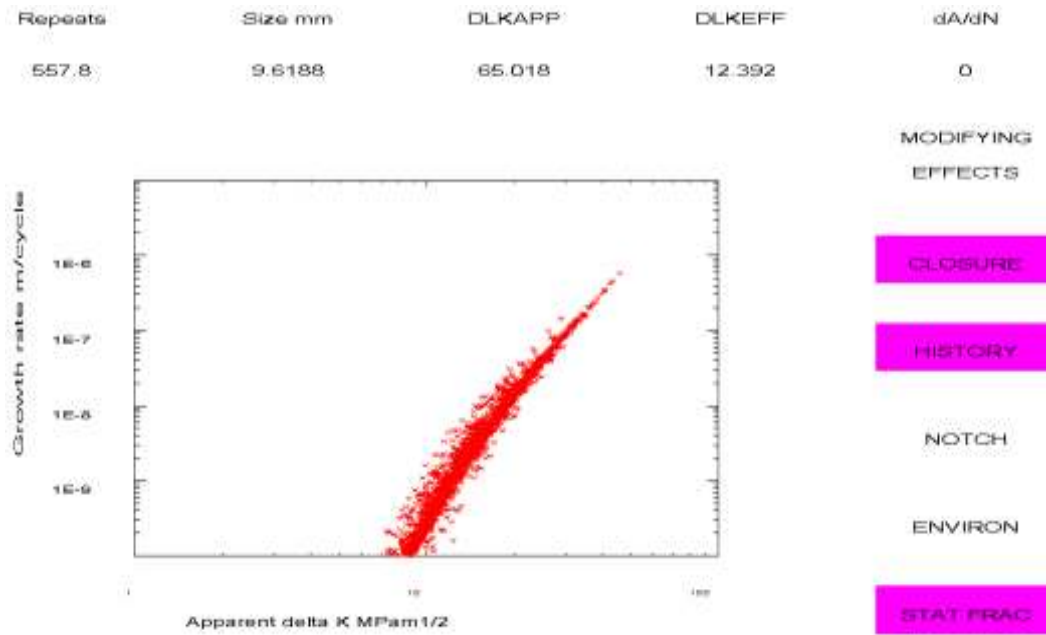
Figure 4.9: The generated crack growth curve under 8kN loading
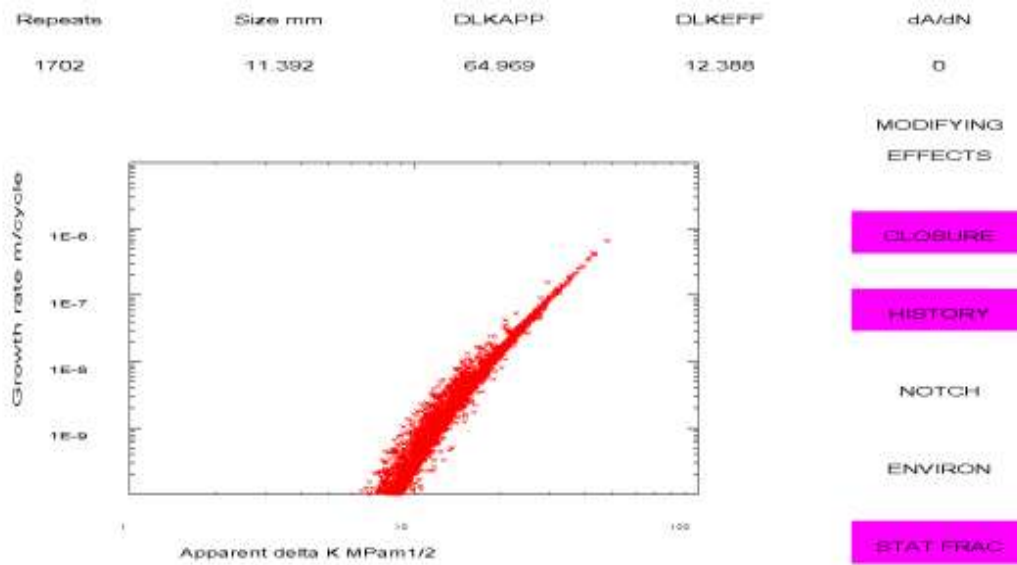
Figure 4.10: The generated crack growth curve under 6kN loading

Repeats	Size mm	DLKAPP	DLKEFF	dA/dN
8158	12	36.085	31.943	1.9491E-7

MODIFYING

EFFECTS

CLOSURE

HISTORY

NOTCH

ENVIRON

STAT FRAC

Growth rate m/cycle

1E-6
1E-7
1E-8
1E-9

Apparent delta K MPam1/2
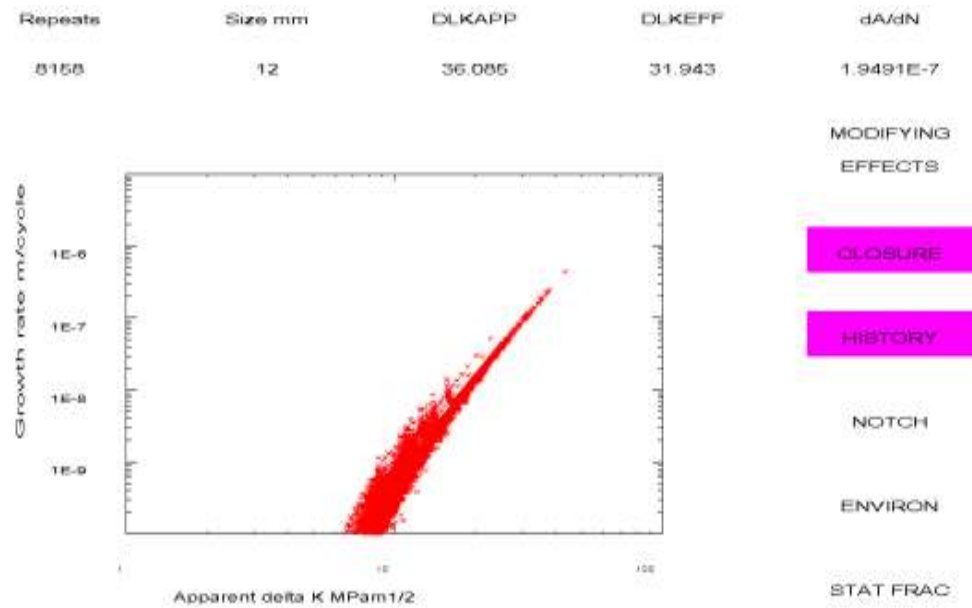
Figure 4.11: The generated crack growth curve under 4kN loading

PCPOST

Equiv. Lif Repeats	Life Cycles	Crack size mm	Stress ran MPa	Apparent d MPam1/2
0	0	2.54	0	0
0.099761	125	2.5752	56.076	40.02
0.19952	250	2.6055	54.361	38.902
0.29928	375	2.6235	29.949	21.467
0.39904	500	2.6433	23.499	16.874
0.4988	625	2.6597	36.161	26.003
0.59856	750	2.68	37.373	26.923
0.69832	875	2.6988	22.592	16.302
0.79808	1000	2.7145	23.197	16.762
0.89785	1125	2.7407	25.214	18.261
0.99761	1250	2.7737	26.413	19.184
1.0974	1375	2.8108	31.39	22.872
1.1971	1500	2.8433	26.727	19.528
1.2969	1625	2.8629	32.461	23.758
1.3966	1750	2.8843	29.925	21.942

End   Up   More   Help

Figure 4.12: Data based on the generated crack growth curve 10kN load

There are also some steps to prove that simulations are running under certain condition. All the required data inserted based on the specification. To plot the Crack growth graph, there are some options we need to follow and analyze.
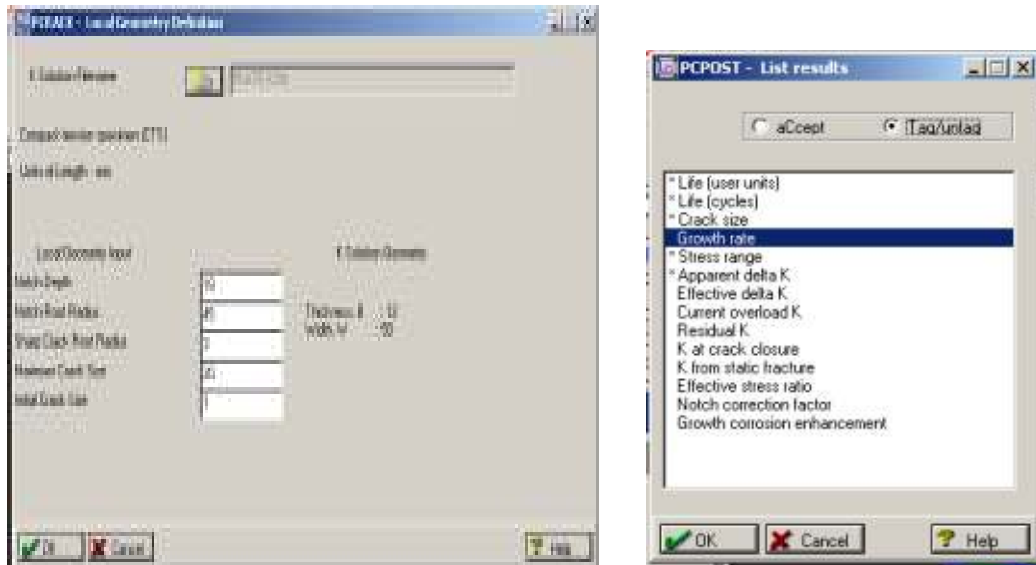
Figure 4.13: Example of step to generated crack growth curve

Overall results for all the simulation using variables axial loads are conclude in the table below. This will make the data collected clearer to analyzed and conclude.

Table 4.1: Data from the linear static analysis

Load (kN)	Displacement (mm)	Stress (MPa)	Strain	Safety Factor
10	3.38	0.23	2.96	1.43
8	2.72	0.17	2.14	2.03
6	2.03	0.13	1.59	2.74
4	1.36	0.08	1.07	4.98

Table 4.2: Data from the analysis of fatigue crack growth curve

Load (kN)	Life Cycles (N)	Crack Size (mm)	Δk Threshold (MPa$\sqrt{m}$)	Δk Critical (MPa$\sqrt{m}$)
10	690972	8.11	12.57	66.09
8	1655572	9.62	12.39	65.02
6	5050964	11.39	12.38	64.97
4	5594108	12.00	-	-

4.4   FATIGUE LIFE PREDICTION

S-N Curve will be determined using manual calculation by using the modified Paris Law Equation. The collected data will arrange in the table with the formula. Based on the journal, all material has their initial crack even before applied static load or cyclic load. This initial crack is very small, and has been assumed in calculation according to the material. From the calculation, the Y-axis intercept, C and the gradient of the straight line, m is determined, and inserted in the table.

4.4.1   Sample of Calculation

Next calculation will focus on stress intensity factor and also the life cycle, N. Then, the S-N curve will be constructed in term of maximum stress and life cycle. Equation 4.1 show the modified Paris Law used in the manual calculation for the S-N curve. Detail calculations are shown in appendix C which is using Microsoft Excel. Overall calculations are based on values from the equation below, which is show already in chapter 2.

$$\frac{da}{dN} = C(\Delta K^m - \Delta K_{th}{}^m)$$

(4.1)

Based on the numerical method calculations, the Y axis intercept and gradient of the crack growth curve are determined as C = 1.2 E-10 and m = 4.06. Only one load selected, which is 10kN for manual calculation as long as the final S-N curve for aluminium alloys are constant eventhough use different load. The value of endurance limit also determined and the value is constant based on aluminium alloy AA1060.

4.4.2 S-N Curve Prediction

Table 4.2: The values of all variable stress ranges and total life

Stress Range, $\Delta\sigma$ (MPa)	Total Life, ΔN
1200	935
1000	1649
800	3658
600	10374
400	46139
200	127918
100	789555
95	1458499
90	679044

From the table above, it shows that the material has been achieve the endurance limit, where the value of total life decrease even the stress also increase. This situation proves that there is no failure in the aluminium alloy under stress 47MPa.
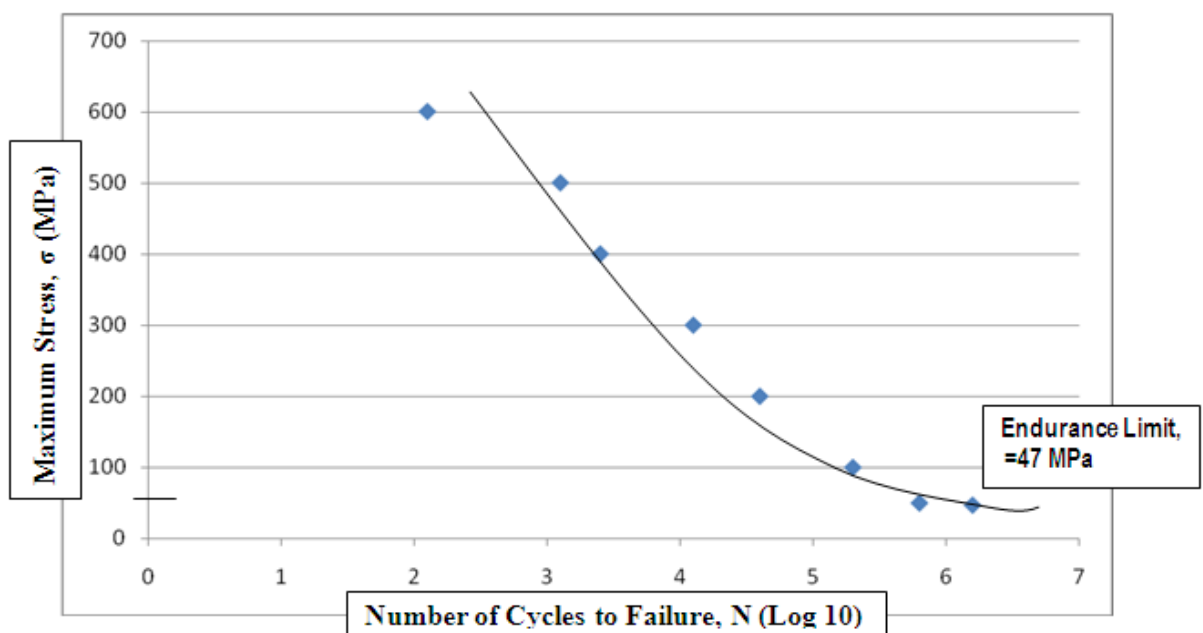
Figure 4.14: S-N curve for the aluminium alloy under 10kN cyclic loading

CHAPTER 5

CONCLUSION AND RECOMMENDATIONS

5.1 CONCLUSION

The main objective of this project is simulating to produce generated Crack Growth Rate graph from the fatigue analysis using MSC PATRAN, with MSC NASTRAN and MSC FATIGUE as solver. From the variable loads applied, the graphs have been successfully constructed. These results have proved that fatigue analysis can be run properly using MSC PATRAN analysis. Besides from tools experimental values, fatigue life of materials also can be predicted from software simulation. The effects of cyclic loading under Mode I also can be analyzed from the Crack Growth graph.

Second objective also have been achieved from this project, which is determining the values of stress intensity factor range ΔK, for both point. At threshold point, stress intensity factor seems to be changed proportional to the axial load applied. For the critical point, the stress intensity is acceptable according to the rate of crack growth respect to the number of load cycles number. For the 10kN applied load, the stress intensity factor at threshold point is approximately 12.57MPa√m. For the critical point, the stress intensity factor is approximately 66.09 MPa√m. For 8kN applied axial load, the stress intensity factor at threshold is approximately 12.39 MPa√m. For critical point, the stress intensity factor is approximately 65.02 MPa√m. Third simulation which use 6kN load, show the threshold stress intensity factor approximately 12.38 MPa√m, and at critical point stress intensity approximately 64.97 MPa√m.

Last simulation which use 4 kN axial load have a undefined results, because the load is small, and take a very long time to display the results. Created S-N Curve from

manual calculation using Modified Paris law, has shown the crack propagation or growth rate of aluminium alloy will be faster if the load applied is increased. This is common situation for all material, except for the value from the S-N Curve. Finally, the endurance limit of aluminium alloy has been determined as 47 MPa. This is because the value of total life decrease, and shown that the material has failed by the repeated load.

Besides that, there is important information stated from the S-N Curve. Log Cycle (Life) ΔN, for each axial loadings applied that in cyclic form is different. From the initial simulation that use 10kN load, the life of aluminium alloy is shorter compared to smaller load applied, which is decreasing every 2kN. In this project, 4kN axial load applied have the longest life. In conclusion, bigger load applied to the model, the Log Cycle (Life) of the material will be decreased. It proved that life of the material is inversely proportional to the amount of load exerted.

Since this simulation fixes the maximum crack propagation value, the load will repeat until the maximum crack achieved. Different load will repeat in different number until the final propagation point. All the values can be observed in the results obtained. Bigger load will repeat less number cyclically. In the other hand, numbers of repeated loads also have clear effects in this fatigue life simulation. If the load is constant and final propagation value not fixed, the repeated condition will be the main parameter in determining the life of aluminium alloy. It will state as the bigger cyclically repeated load will have longer crack propagation. That why we come out with this analysis and simulation, to predict fatigue life of the material.
.

5.2 RECOMMENDATIONS

Fatigue analysis not necessarily follows the same design and model as used in simulation. Compact Tension Specimen can be replaced with other model of experimental or stimulation, especially Keyhole model. Compact Tension Specimen used because it quite easy to run under Mode 1and produces consistent results. Dimension of the model used also exchangeable. There are no limit in determine the
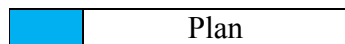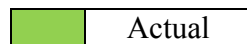
dimension, but for the most common, this software simulation using a specified dimension used in previous research and experiments.

In the analysis, other results also can be produced from MSC FATIGUE such as S-N curve and E-N curve. This graph is important for the prediction of fatigue life for any materials. While using the single load, or variable loads, the steps to produce these graphs is not really different from Crack Growth graph. The data collected can be useful for the future research and experiment in fatigue life prediction. In addition, the results and graphs also can be used in manufacturing process especially in case of material selection.

Besides, analysis of fatigue life prediction also can be done using Mode II and Mode III. The final result is approximately same with Mode I, except the applied load. There are different directions shear and force exerted on the model if we use Mode II and Mode III. These types of Mode are available according to the need of the parts we used. Using this software simulation also available with static loading or repeated loading, but researcher prefer repeated loading because common uses material is related to repeated or cyclic loading. Other materials are also acceptable for the simulations using MSC PATRAN and MSC FATIGUE. For the base material, researcher always uses common metal especially stainless steel and aluminium alloy. There are so many material that we can choose from the options.

APPENDIX D1

PROJECT ACTIVITIES	WEEKS													
	1	2	3	4	5	6	7	8	9	10	11	12	13	14
Identify project	▓	▓	▓											
					▓	▓								
Project briefing			▓	▓	▓	▓								
						▓	▓							
Literature review				▓	▓	▓	▓	▓	▓					
								▓	▓	▓	▓			
Determine methodology										▓	▓	▓		
												▓	▓	
Proposal writing							▓	▓	▓	▓	▓	▓		
								▓	▓	▓	▓	▓	▓	
Submit proposal													▓	
														▓
Presentation preparation													▓	
													▓	▓
Present proposal														▓
														▓

■ Plan   ■ Actual

Figure 6.5: Final Year Project (FYP) I

APPENDIX D2

PROJECT ACTIVITIES	WEEKS																						
	1	2	3	4	5	6	7	8	9	10	11	12	13	14	15	16	17	18	19	20	21	22	23
Design control scheme (Plan)	■	■	■																				
Design control scheme (Actual)	■	■	■	■	■																		
Run simulation and evaluate result (Plan)				■	■	■	■	■	■	■													
Run simulation and evaluate result (Actual)				■	■	■	■	■	■	■	■												
Comparative study/discussion (Plan)											■	■											
Comparative study/discussion (Actual)											■	■											
conclusion (Plan)													■										
conclusion (Actual)													■										
submit Draft I (Plan)														■	■								
submit Draft I (Actual)														■									
Submit draft II and log book (Plan)																■							
Submit draft II and log book (Actual)																■							
Correction final draft (Plan)																		■	■				
Correction final draft (Actual)																		■	■	■	■		
Approval Document (Plan)																				■	■		
Approval Document (Actual)																					■		
FYP presentation (Plan)																						■	
FYP presentation (Actual)																						■	
Hard binding and submit thesis (Plan)																							■
Hard binding and submit thesis (Actual)																							■

■ Plan   ■ Actual

Figure 6.6: Final Year Project (FYP) II

REFERENCES

The information and factual data were referred from the following reference:

C. L. Chow, X. F. Chen. 1993. Failure Analysis of a Cracked Plate Based on Endochronic Plastic Theory Coupled With Damage. International Journal of Fracture 60.49-63.

C.T.F. Ross. 1986. Finite Element Programs for Axisymmetric Problems in Engineering.Finite Elements in Analysis and Design 2. Wiley & Sons Publisher. 327-331.

David S. Jacobs, I-Wei Chen. 1994. Mechanical and Environmental Factors in the Cyclic and Static Fatigue of Silicon Nitride. Journal of Ceramic Society.53-61.

D. H. Kohn, P. Ducheyne, J. Awerbuch. 1992. Acoustic Emission During Fatigue of Ti-6AI-4V: Incipient Fatigue Crack Detection Limits and Generalized Data Analysis Methodology. Journal of Materials Science, 27. 3133-3142.

Divesh Bhatt, Ahren W. Jasper, Nathan E. Schultz, J. Ilja Siepmann, Donald G. Truhlar.2005. Critical Properties of Aluminium. Journal of America Chemistry Society,128. 4224 4225.

D. J. Morrison. J. W. Jones, D. E. Alexander. 1989. The Effect of Ion Beam Surface Modifications on Fatigue Crack Initiation in Polycrystalline Nickel. Materials Science and Engineering, A 115. 315-321.

D. L. Li, C. L. Chow. 1993. A Damage Mechanics Approach to Fatigue Assessment in Offshore Structures. 385 International Journal of Damage Mechanics, Vol. 2. Technomic Publishing Co. Inc. 385

E H Lee, R.L. Mallet, W H Yang. 1974. Dynamic Analysis of Structural Deformation and Metal Forming. Computer Methods in Applied Mechanics and Engineering 5. North Holland Publishing Company.69-82.

G. M. Vyletel, D. C. Van Aken, J. E. Allison. 1991. Effect of Microstructure on the Cyclic Response and Fatigue Behavior of an Aluminum Metal Matrix Composite. Vol. 25, pp. 2405-2410.

J. Huang, J. E. Spowart, J. W. Jones. 2006. Fatigue Behaviour of SiCp-Reinforced Aluminium Composites in the Very High Cycle Regime Using Ultrasonic Fatigue.

Kamel Makhlouf, J. W. Jones. 1992. Near-Threshold Fatigue Crack Growth Behaviour of a Ferritic Stainless Steel at Elevated Temperatures. International Journal of Fatigue 14, No 2. pp 97-104.

Kevin J Elwood, T. C. Papanastasiou, J. O. Wilkies. 1992. Three Dimensional Streamlined Finite Elements: Design of Extrusions Dies. International Journal for Numerical Method in Fluids, Vol. 14, 13-24.

L. J. Doctors. 1970. An Application of the Finite Element Technique to Boundary Value Problems of Potential Flow. International Journal for Numerical Methods in Engineering. Vol. 2. 243-252.

L. Wang, S.R. Daniewicz, M.F. Horstemeyer, S. Sintay, A.D. Rollett. 2009. Three- Dimensional Finite Element Analysis Using Crystal Plasticity for a Parameter Study of Microstructurally Small Fatigue Crack Growth in AA7075 Aluminum Alloy. International Journal of Fatigue,31. 651–658.

Nam H. Kim, Kyung K. Choi, Jun Dong, Christophe Pierre. 2003. Design Optimization of Structural Acoustic Problems Using FEM-BEM

Noboru Kikuchi, Kyoon Yang Chung, Toshikazu Torigaki, John E. Taylor. 1986. Adaptive Finite Element Method for Shape Optimization of Linearly Elastic Structure. Computer Method in Applied Mechanics and Engineering, 57. 67-89

R. J. Lomax. 1977. Preservation of the Conservation Properties of the Finite Element Method Under Local Mesh Refinement. Computer Methods in Applied Mechanics and Engineering, 12. 309-314.

R. S. Rao and H. Y. Lee. 1989. A Finite Element Solution of Strip Rolling. Journal of Mechanics Working Technology, 20. Science Publishers B.V, Amsterdam. 453-461.

S. Ishihara, A.J. McEvily. 2002. Analysis of Short Fatigue Crack Growth in Cast Aluminium Alloys. International Journal of Fatigue, 24. 1169–1174.

T. K. Brog, J. W. Jonesi, G. S. Wass. 1984. Fatigue Crack Growth Retardation Inconel 600. Engineering Fracture Mechanics, Vol. 20, No. 2. 313-320.

Y. W. Mai, A. G. Atkins, R. M. Caddell. 1976. Determination of Valid R-Curves for Materials With Large Fracture Toughness to Yield Strength Ratios. International Journal of Fracture, Vol. 12, No. 3. Noordhoff International Publishing. 391-407.

APPENDIX A

SOLIDWORKS DRAWING
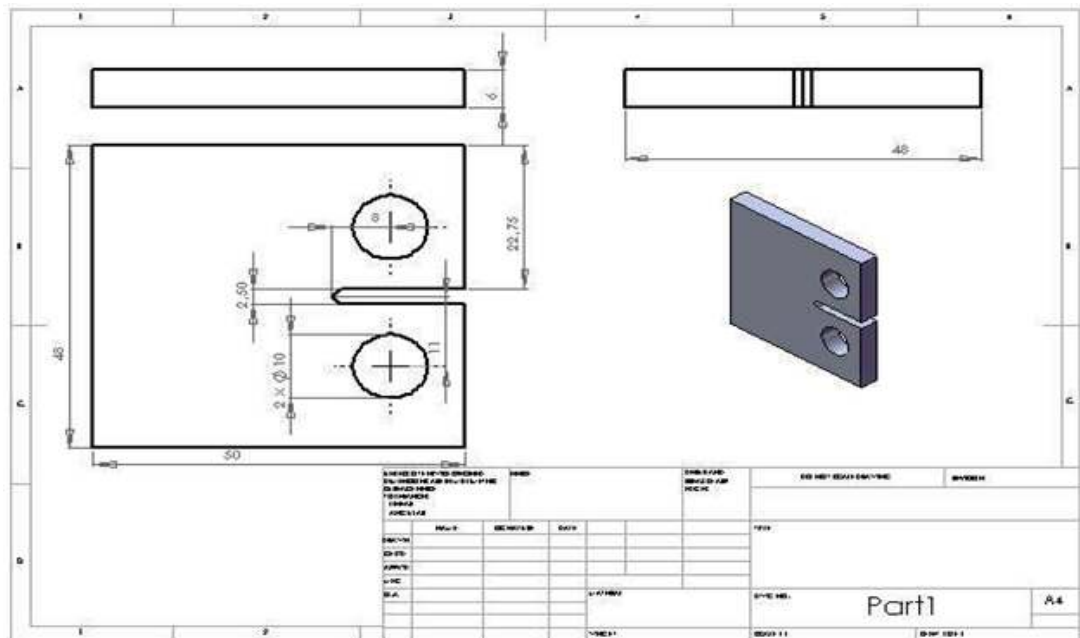
Figure 6.1: SOLIDWORKS drawing for the compact tension model.
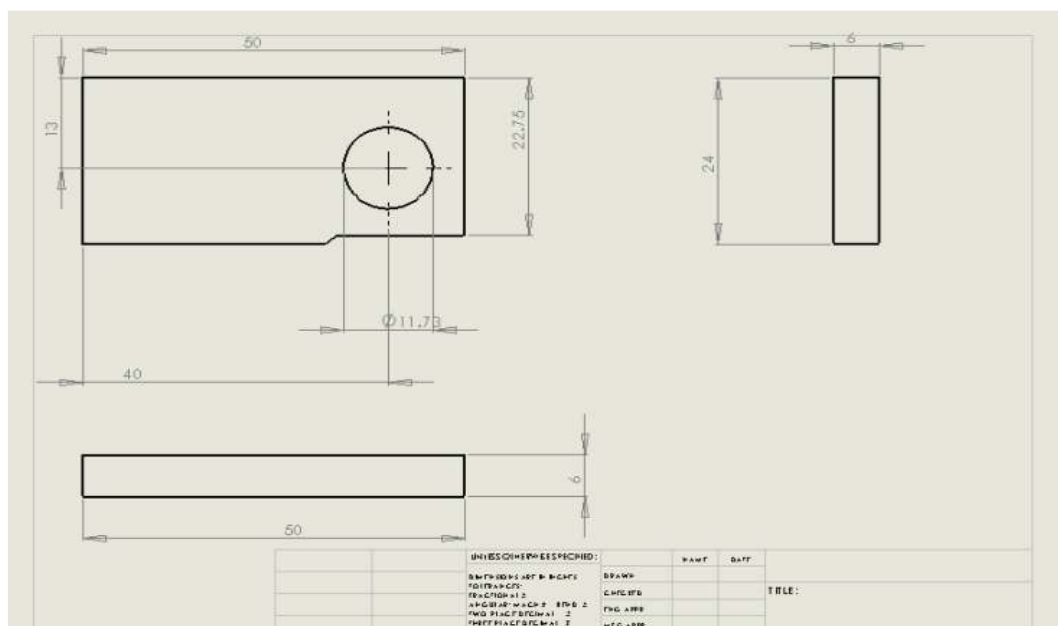
Figure 6.2: SOLIDWORKS drawing for half of the model used in simulation.

APPENDIX B

TABLE OF CALCULATION

	A	B	C	D	E	F	G	H	I
1	CT Specimen R=-1								
2									
3	da/dN	ΔK	Log(da/dN)	Log(ΔK)	Log(ΔK)^2	Log(ΔK)*Log(da/dN)			
4	1.54E-07	16.30	-6.812	1.212	1.4685	-8.252			
5	1.58E-07	16.87	-6.800	1.227	1.5061	-8.345			
6	2.10E-07	18.26	-6.679	1.262	1.5814	-8.425			
7	2.64E-07	19.18	-6.578	1.283	1.6457	-8.439			
8	2.64E-07	21.47	-6.578	1.332	1.7738	-8.761			
9	2.97E-07	22.87	-6.527	1.359	1.8476	-8.872			
10	3.22E-07	23.76	-6.492	1.376	1.8930	-8.932			
11	5.10E-07	26.00	-6.292	1.415	2.0021	-8.904			
12	5.48E-07	26.92	-6.261	1.430	2.0451	-8.854			
13	7.78E-07	28.32	-6.109	1.452	2.1086	-8.871			
14	8.10E-07	31.54	-6.092	1.499	2.2466	-9.130			
15	9.22E-07	32.29	-6.035	1.509	2.2773	-9.108			
16	9.43E-07	34.01	-6.025	1.532	2.3458	-9.229			
17	9.49E-07	35.88	-6.023	1.555	2.4176	-9.364			
18			-89.305	19.442	27.1701	-123.587			
19									
20							m	Log C	C
21							4.06	-9.93	1.2E-10

Figure 6.3: Least Square Method to determine gradient and Y axis intercept

APPENDIX C

(a) Stress Range = 90 Mpa

a	(a/w)	f(a/w)	Δσ	ΔK	da/dN	ΔN
50	0.001	1.784821	90	2.013377	-5.6E-10	-177520
150	0.003	1.810441	90	3.537331	-4.6E-10	-215067
250	0.005	1.836035	90	4.631232	-2.8E-10	-352941
350	0.007	1.861602	90	5.556054	-1.6E-11	-6281629
450	0.009	1.887143	90	6.386407	3.43E-10	291699
550	0.011	1.912657	90	7.155898	8E-10	125023.4
650	0.013	1.938146	90	7.882951	1.36E-09	73363.44
750	0.015	1.96361	90	8.578896	2.04E-09	48992.37
850	0.017	1.989048	90	9.251248	2.84E-09	35170.42
950	0.019	2.014462	90	9.905272	3.78E-09	26459
1050	0.021	2.039851	90	10.54481	4.86E-09	20576.29
1150	0.023	2.065216	90	11.17275	6.1E-09	16404.56
1250	0.025	2.090557	90	11.79133	7.5E-09	13335.71
1350	0.027	2.115875	90	12.40231	9.08E-09	11012.7
1450	0.029	2.14117	90	13.00711	1.09E-08	9213.406
1550	0.031	2.166442	90	13.60688	1.28E-08	7793.133
1650	0.033	2.191692	90	14.20258	1.5E-08	-109793
						679043.4

(b) Stress Range = 95 Mpa

a	(a/w)	f(a/w)	Δσ	ΔK	da/dN	ΔN
50	0.001	1.784821	95	2.125232	-5.6E-10	-178555
150	0.003	1.810441	95	3.733849	-4.4E-10	-226778
250	0.005	1.836035	95	4.888523	-2.2E-10	-452474
350	0.007	1.861602	95	5.864724	1.03E-10	972616.7
450	0.009	1.887143	95	6.741208	5.37E-10	186141.1
550	0.011	1.912657	95	7.553448	1.09E-09	91687.19
650	0.013	1.938146	95	8.320893	1.77E-09	56411.16
750	0.015	1.96361	95	9.055501	2.59E-09	38553.67
850	0.017	1.989048	95	9.765206	3.57E-09	28049.23
950	0.019	2.014462	95	10.45556	4.7E-09	21282.2
1050	0.021	2.039851	95	11.13063	6.01E-09	16646.63
1150	0.023	2.065216	95	11.79345	7.5E-09	13326.53
1250	0.025	2.090557	95	12.4464	9.2E-09	10866.57
1350	0.027	2.115875	95	13.09132	1.11E-08	8994.464
1450	0.029	2.14117	95	13.72972	1.33E-08	7538.439
1550	0.031	2.166442	95	14.36282	1.57E-08	6385.427
1650	0.033	2.191692	95	14.99161	1.83E-08	-90063
						1458499

(c) Stress Range = 100 Mpa

a	(a/w)	f(a/w)	Δσ	ΔK	da/dN	ΔN
50	0.001	1.784821	100	2.237086	-5.56319E-10	-179753
150	0.003	1.810441	100	3.930368	-4.13514E-10	-241830
250	0.005	1.836035	100	5.145814	-1.49768E-10	-667701
350	0.007	1.861602	100	6.173394	2.38531E-10	419232.9
450	0.009	1.887143	100	7.096008	7.59437E-10	131676.5
550	0.011	1.912657	100	7.950998	1.42307E-09	70270.64
650	0.013	1.938146	100	8.758834	2.2409E-09	44624.89
750	0.015	1.96361	100	9.532107	3.22548E-09	31003.18
850	0.017	1.989048	100	10.27916	4.39026E-09	22777.71
950	0.019	2.014462	100	11.00586	5.74957E-09	17392.61
1050	0.021	2.039851	100	11.71645	7.31855E-09	13663.9
1150	0.023	2.065216	100	12.41416	9.11315E-09	10973.16
1250	0.025	2.090557	100	13.10147	1.11501E-08	8968.545
1350	0.027	2.115875	100	13.78034	1.34469E-08	7436.674
1450	0.029	2.14117	100	14.45234	1.60218E-08	6241.484
1550	0.031	2.166442	100	15.11875	1.88941E-08	5292.665
1650	0.033	2.191692	100	15.78064	2.20835E-08	-74716.3
						789554.8

(d) Stress Range = 200 Mpa

a	(a/w)	f(a/w)	Δσ	ΔK	da/dN	ΔN
50	0.001	1.784821	200	4.474172	-3.17304E-10	-315155
150	0.003	1.810441	200	7.860735	1.34377E-09	74417.33
250	0.005	1.836035	200	10.29163	4.41162E-09	22667.42
350	0.007	1.861602	200	12.34679	8.92822E-09	11200.44
450	0.009	1.887143	200	14.19202	1.49873E-08	6672.321
550	0.011	1.912657	200	15.902	2.27065E-08	4404.023
650	0.013	1.938146	200	17.51767	3.22194E-08	3103.724
750	0.015	1.96361	200	19.06421	4.36717E-08	2289.812
850	0.017	1.989048	200	20.55833	5.72202E-08	1747.635
950	0.019	2.014462	200	22.01171	7.30314E-08	1369.274
1050	0.021	2.039851	200	23.4329	9.12815E-08	1095.512
1150	0.023	2.065216	200	24.82833	1.12156E-07	891.6168
1250	0.025	2.090557	200	26.20295	1.35849E-07	736.1116
1350	0.027	2.115875	200	27.56068	1.62565E-07	615.1396
1450	0.029	2.14117	200	28.90468	1.92516E-07	519.4371
1550	0.031	2.166442	200	30.23751	2.25925E-07	442.624
1650	0.033	2.191692	200	31.56128	2.63024E-07	-6273.18
						132172.4

(e) Stress Range = 400 Mpa

a	(a/w)	f(a/w)	Δσ	ΔK	da/dN	ΔN
50	0.001	1.784821	400	8.948344	2.46287E-09	40603.02
150	0.003	1.810441	400	20.58325	5.74686E-08	1740.079
250	0.005	1.836035	400	24.69357	1.10005E-07	909.0515
350	0.007	1.861602	400	24.69357	1.10005E-07	909.0515
450	0.009	1.887143	400	28.38403	1.80483E-07	554.0703
550	0.011	1.912657	400	31.80399	2.70271E-07	369.9992
650	0.013	1.938146	400	35.03534	3.80922E-07	262.5208
750	0.015	1.96361	400	38.12843	5.14133E-07	194.5021
850	0.017	1.989048	400	41.11666	6.71726E-07	148.8702
950	0.019	2.014462	400	44.02343	8.55639E-07	116.8717
1050	0.021	2.039851	400	46.86581	1.06792E-06	93.63998
1150	0.023	2.065216	400	49.65665	1.31073E-06	76.29363
1250	0.025	2.090557	400	52.40589	1.58632E-06	63.03902
1350	0.027	2.115875	400	55.12137	1.89707E-06	52.71285
1450	0.029	2.14117	400	57.80937	2.24546E-06	44.53433
1550	0.031	2.166442	400	60.47502	2.63407E-06	37.96409
1650	0.033	2.191692	400	63.12256	3.06559E-06	
						46138.26

(f) Stress Range = 600 Mpa

a	(a/w)	f(a/w)	Δσ	ΔK	da/dN	ΔN
50	0.001	1.784821	600	13.42252	1.21996E-08	8197.012
150	0.003	1.810441	600	23.58221	9.33702E-08	1071.005
250	0.005	1.836035	600	30.87488	2.43284E-07	411.0417
350	0.007	1.861602	600	37.04036	4.63994E-07	215.5201
450	0.009	1.887143	600	42.57605	7.60078E-07	131.5655
550	0.011	1.912657	600	47.70599	1.13729E-06	87.9285
650	0.013	1.938146	600	52.55301	1.60215E-06	62.41631
750	0.015	1.96361	600	57.19264	2.16178E-06	46.25821
850	0.017	1.989048	600	61.67499	2.82384E-06	35.41274
950	0.019	2.014462	600	66.03514	3.59648E-06	27.80498
1050	0.021	2.039851	600	70.29871	4.48829E-06	22.28019
1150	0.023	2.065216	600	74.48498	5.50834E-06	18.15428
1250	0.025	2.090557	600	78.60884	6.66614E-06	15.00119
1350	0.027	2.115875	600	82.68205	7.97164E-06	12.54447
1450	0.029	2.14117	600	86.71405	9.43525E-06	10.59855
1550	0.031	2.166442	600	90.71253	1.10678E-05	9.035189
1650	0.033	2.191692	600	94.68383	1.28807E-05	-128.098
						10373.58

(g) Stress Range = 800 Mpa

a	(a/w)	f(a/w)	Δσ	ΔK	da/dN	ΔN
50	0.001	1.784821	800	17.89669	3.48013E-08	2873.46
150	0.003	1.810441	800	31.44294	2.59542E-07	385.2939
250	0.005	1.836035	800	41.16651	6.74616E-07	148.2324
350	0.007	1.861602	800	49.38715	1.2857E-06	77.77834
450	0.009	1.887143	800	56.76807	2.10549E-06	47.49496
550	0.011	1.912657	800	63.60798	3.14988E-06	31.74719
650	0.013	1.938146	800	70.07068	4.43696E-06	22.53797
750	0.015	1.96361	800	76.25685	5.98644E-06	16.70442
850	0.017	1.989048	800	82.23332	7.81953E-06	12.7885
950	0.019	2.014462	800	88.04686	9.95876E-06	10.04141
1050	0.021	2.039851	800	93.73162	1.2428E-05	8.046371
1150	0.023	2.065216	800	99.3133	1.52522E-05	6.556421
1250	0.025	2.090557	800	104.8118	1.84579E-05	5.417744
1350	0.027	2.115875	800	110.2427	2.20725E-05	4.530532
1450	0.029	2.14117	800	115.6187	2.61248E-05	3.827775
1550	0.031	2.166442	800	120.95	3.06451E-05	3.263169
1650	0.033	2.191692	800	126.2451	3.56645E-05	-46.2645
						3657.721

(h) Stress Range = 1000 Mpa

a	(a/w)	f(a/w)	Δσ	ΔK	da/dN	ΔN
50	0.001	1.784821	1000	22.37086	7.73719E-08	1292.459
150	0.003	1.810441	1000	39.30368	5.7253E-07	174.6635
250	0.005	1.836035	1000	51.45814	1.48704E-06	67.24783
350	0.007	1.861602	1000	61.73394	2.83341E-06	35.29315
450	0.009	1.887143	1000	70.96008	4.63958E-06	21.55365
550	0.011	1.912657	1000	79.50998	6.94064E-06	14.40789
650	0.013	1.938146	1000	87.58834	9.77637E-06	10.22875
750	0.015	1.96361	1000	95.32107	1.31902E-05	7.581358
850	0.017	1.989048	1000	102.7916	1.7229E-05	5.804176
950	0.019	2.014462	1000	110.0586	2.19422E-05	4.557425
1050	0.021	2.039851	1000	117.1645	2.73825E-05	3.651973
1150	0.023	2.065216	1000	124.1416	3.3605E-05	2.97575
1250	0.025	2.090557	1000	131.0147	4.06678E-05	2.458949
1350	0.027	2.115875	1000	137.8034	4.86316E-05	2.056276
1450	0.029	2.14117	1000	144.5234	5.75599E-05	1.73732
1550	0.031	2.166442	1000	151.1875	6.75191E-05	1.481063
1650	0.033	2.191692	1000	157.8064	7.8578E-05	-20.9982
						1648.158

(i) Stress Range = 1200 MPa

a	(a/w)	f(a/w)	Δσ	ΔK	da/dN	ΔN
50	0.001	1.784821	1200	26.84503	1.48056E-07	675.4185
150	0.003	1.810441	1200	47.16441	1.09222E-06	91.55703
250	0.005	1.836035	1200	61.74976	2.83598E-06	35.26113
350	0.007	1.861602	1200	47.16441	1.09222E-06	91.55703
450	0.009	1.887143	1200	85.1521	8.84721E-06	11.30299
550	0.011	1.912657	1200	95.41197	1.32348E-05	7.555818
650	0.013	1.938146	1200	105.106	1.8642E-05	5.364244
750	0.015	1.96361	1200	114.3853	2.51515E-05	3.975908
850	0.017	1.989048	1200	123.35	3.28525E-05	3.043911
950	0.019	2.014462	1200	132.0703	4.18396E-05	2.39008
1050	0.021	2.039851	1200	140.5974	5.2213E-05	1.915233
1150	0.023	2.065216	1200	148.97	6.4078E-05	1.560599
1250	0.025	2.090557	1260	165.0786	9.21649E-05	1.085012
1350	0.027	2.115875	1260	173.6323	0.000110213	0.907333
1450	0.029	2.14117	1260	182.0995	0.000130447	0.766594
1550	0.031	2.166442	1260	190.4963	0.000153017	0.653521
1650	0.033	2.191692	1260	198.8361	0.00017808	
						934.3149

Figure 6.4: Manual calculation for S-N curve after using Modified Paris Law Equation